Available online at www.sciencedirect.com
SCIENCE DIRECT®
Journal of Sound and Vibration 292 (2006) 21–58
JOURNAL OF SOUND AND VIBRATION
www.elsevier.com/locate/jsvi

On the modal damping ratios of shear-type structures equipped with Rayleigh damping systems

T. Trombetti*, S. Silvestri

DISTART, Facoltà di Ingegneria, Università degli Studi di Bologna, Viale Risorgimento 2, 40136 Bologna, Italy

Received 29 July 2002; received in revised form 6 July 2005; accepted 15 July 2005
Available online 28 September 2005

Abstract

The effects of added manufactured viscous dampers upon shear-type structures are analytically investigated here for the class of Rayleigh damping systems. The definitions of mass proportional damping (MPD) and stiffness proportional damping (SPD) systems are briefly recalled and their physical counterpart is derived. From basic physics, a detailed mathematical demonstration that the first modal damping ratio of a structure equipped with the MPD system is always larger than the first modal damping ratio of a structure equipped with the SPD system is provided here. All results are derived for the class of structures characterised by constant values of lateral stiffness and storey mass, under the equal "total size" constraint. The paper also provides closed form demonstrations of other properties of modal damping ratios which further indicate that the MPD and the SPD systems are respectively characterised by the largest and the smallest damping efficiency among Rayleigh damping systems subjected to base excitation. A numerical application with realistic data corresponding to an actual seven-storey building structure is presented to illustrate and verify the theoretical findings.

1. Introduction

Dissipative systems have widely proven their effectiveness in mitigating seismic effects in shear-type structures and have been the object of many research works [1–9]. Still the issue is open in

*Corresponding author. Tel.: +39 051 209 3242; fax: +39 051 209 3236.
E-mail addresses: tomaso.trombetti@mail.ing.unibo.it (T. Trombetti), stefano.silvestri@mail.ing.unibo.it (S. Silvestri).

0022-460X/$ - see front matter © 2005 Elsevier Ltd. All rights reserved.
doi:10.1016/j.jsv.2005.07.023

terms of identifying the additional damper system that maximises the overall dissipative properties of the structure under a wide range of dynamic inputs and with reference to various performance indexes. In fact, for shear-type structures, several research works have proposed algorithms for the numerical identification of the damper system, often referred to as "optimal" damper system, that optimises the performances with reference to (a) a selected performance index, (b) a given dynamic input and (c) a specific structure. The validity of these works resides mainly in the formulation of the optimisation algorithms.

Furthermore, in the body of the up to date researches available in literature, the search for the "optimal" damper system takes into consideration only dampers positioned between adjacent storeys, thus neglecting other arrangements technically and physically implementable in shear-type structures. For example, the "Osaka International Convention Center" [10,11] (in Osaka, Japan, completed in 2000) and the "Wallace Bennett Federal Building" [12–14] (in Salt Lake City, USA, completed in 2002) make use of dissipative devices that connect non-adjacent storeys.

In this work, the authors aim at identifying the "optimal" damper system through studies based upon the physical properties of Rayleigh damping matrix, taking also in consideration a new way of inserting viscous dampers into structures which sees these devices connecting each storey to a fixed point.

2. The equations of motion for damped shear-type structures

For a generic N-storey linear elastic shear-type frame structure subjected to a dynamic excitation $\mathbf{p}(t)$, the equations of motions can be written, in time domain, as follows [15,16]:

$$\mathbf{M}\ddot{\mathbf{u}}(t) + \mathbf{C}\dot{\mathbf{u}}(t) + \mathbf{K}\mathbf{u}(t) = \mathbf{p}(t), \tag{1}$$

where $\mathbf{M}$ is the mass matrix, $\mathbf{K}$ is the stiffness matrix, $\mathbf{C}$ is the damping matrix and $\mathbf{u}(t)$ is the displacement vector representing the displaced shape of the system, as given in Fig. 1. A dot over a

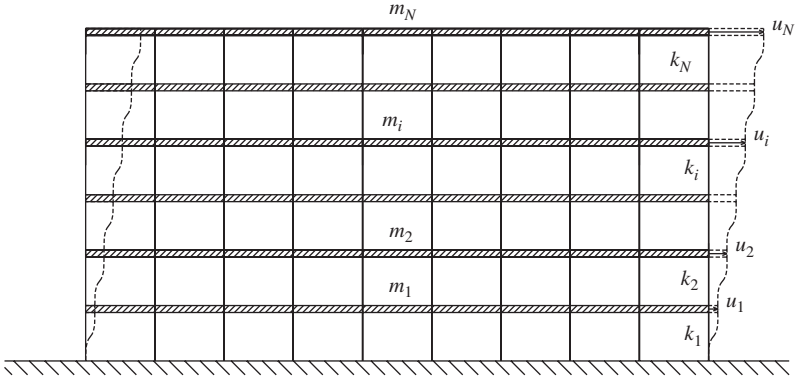

Fig. 1. The generic N-storey linear elastic shear-type frame structure.

symbol indicates differentiation with respect to time. Always with reference to Fig. 1:

$$\mathbf{M} = \begin{bmatrix} m_1 & 0 & \ldots & & & \ldots & 0 \\ 0 & m_2 & 0 & \ldots & & & \ldots \\ \ldots & 0 & \ldots & & & & \\ & & & m_i & & & \\ & & & & \ldots & & \ldots \\ \ldots & & & & & m_{N-1} & 0 \\ 0 & \ldots & & & \ldots & 0 & m_N \end{bmatrix} \tag{2}$$

with m_i representing the mass of the ith storey;

$$\mathbf{K} = \begin{bmatrix} k_1 + k_2 & -k_2 & 0 & \ldots & & & 0 \\ -k_2 & k_2 + k_3 & -k_3 & 0 & \ldots & & \ldots \\ 0 & -k_3 & k_3 + k_4 & \ldots & & & \\ \ldots & & \ldots & \ldots & & & \\ & & & & \ldots & \ldots & 0 \\ \ldots & & & & \ldots & k_{N-1} + k_N & -k_N \\ 0 & \ldots & & & & -k_N & k_N \end{bmatrix} \tag{3}$$

with k_i representing the total lateral stiffness of the vertical elements connecting the ith storey to the (i-1)th storey (to the ground if $i = 1$);

$$\mathbf{u}(t) = \begin{Bmatrix} u_1(t) \\ u_2(t) \\ \ldots \\ u_i(t) \\ \ldots \\ u_N(t) \end{Bmatrix} \tag{4}$$

with $u_i(t)$ being the physical displacement of the ith degree of freedom (as computed with respect to the base, see Fig. 1);

$$\mathbf{p}(t) = \begin{Bmatrix} p_1(t) \\ p_2(t) \\ \ldots \\ p_i(t) \\ \ldots \\ p_N(t) \end{Bmatrix}, \tag{5}$$

where $p_i(t)$ is the dynamic loading acting at the ith degree of freedom.

Note that, given the purposes of the analyses developed in this paper (identification of the "optimal" damper system), the exact form of matrix **C** is still undetermined. In general terms, **C** is a $N \times N$ matrix which can be full, banded or diagonal depending on the system of added viscous dampers which is introduced into the structure:

$$\mathbf{C} = \begin{bmatrix} c_{11} & c_{12} & \dots & c_{1j} & \dots & c_{1N} \\ c_{21} & c_{22} & \dots & c_{2j} & \dots & c_{2N} \\ \dots & \dots & & \dots & & \dots \\ c_{i1} & c_{i2} & & c_{ij} & & c_{iN} \\ \dots & \dots & & \dots & & \dots \\ c_{N1} & c_{N2} & \dots & c_{Nj} & \dots & c_{NN} \end{bmatrix} \tag{6}$$

with c_{ij} representing the force corresponding to degree of freedom i due to unit velocity of degree of freedom j (with all other degrees of freedom having a constant null displacement).

3. The systems of added viscous dampers which lead to Rayleigh damping matrix

In the dynamic systems considered in this paper internal damping is neglected, so that the damping matrix derives from the effects of added viscous dampers only. The added viscous dampers are here modelled by means of a linear force–velocity relationship $F_d = c \cdot v$, where F_d is the force provided by the damper, c is its damping coefficient and v is the relative velocity between the two damper ends.

Let us consider an ensemble (system) of added viscous dampers which leads, for the generic N-storey linear elastic shear-type frame structure described in Section 2, to a Rayleigh damping matrix $\mathbf{C}^R$ [15,16]. The Rayleigh damping matrix has the following expression:

$$\mathbf{C}^R = \alpha\mathbf{M} + \beta\mathbf{K}, \tag{7}$$

where **M** and **K** are, respectively, the mass matrix and the stiffness matrix given in Section 2 and α and β are two constants having, respectively, units of s^{-1} and s.

For the sake of clarity, the system of added viscous dampers defined above is referred herein to as "Rayleigh damping system" and structures characterised by a Rayleigh damping system will be indicated hereafter as "Rayleigh damped" structures. As an illustrative example, Fig. 2 provides the physical representation of a six-storey "Rayleigh damped" shear-type structure. This physical representation is simply obtained from Eq. (7) and from the definition of c_{ij}.

Eq. (7) leads also to the definition of the following two limiting cases:

- a system of added viscous dampers which leads to a damping matrix proportional to the mass matrix only (mass proportional damping matrix—MPD matrix), as given by

$$\mathbf{C}^{\mathrm{MPD}} = \alpha\mathbf{M}. \tag{8}$$

- a system of added viscous dampers which leads to a damping matrix proportional to the stiffness matrix only (stiffness proportional damping matrix—SPD matrix), as given by

$$\mathbf{C}^{\mathrm{SPD}} = \beta\mathbf{K}. \tag{9}$$

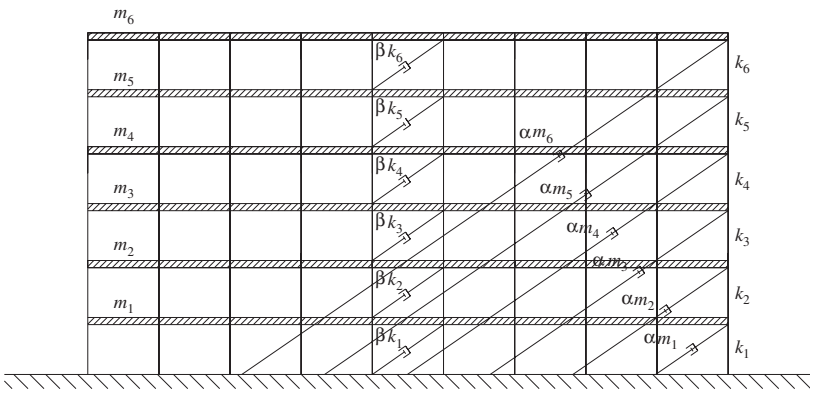

Fig. 2. Six-storey shear-type structure equipped with Rayleigh damping system.

For the sake of clarity, the system of added viscous dampers which leads to an MPD matrix is referred herein to as "MPD system" and structures characterised by an MPD system will be indicated hereafter as "MPD structures". Similarly, the system of added viscous dampers which leads to an SPD matrix is referred herein to as "SPD system" and structures characterised by an SPD system will be indicated hereafter as "SPD structures". As illustrative examples, Figs. 3a and b provide physical representations of a six-storey MPD structure and of a six-storey SPD structure, respectively.

$$\text{Note that } \mathbf{C}^R = \mathbf{C}^{\text{MPD}} + \mathbf{C}^{\text{SPD}}.$$

Inspection of Figs. 3a and b shows that the MPD system and the SPD system correspond to two physically separated and independently implementable damper systems. Note that the dampers of the MPD system (αm_i) link each storey to a fixed point (ground), while the dampers of the SPD system (βk_i) link each storey to the adjacent one. At once, as a result of this new observation, an alternative definition of MPD and SPD systems can be given in terms of damper placement and damper sizing:

- *MPD system*: dampers are placed so that they connect each storey to a fixed point (ground or infinitely stiff vertical lateral-resisting element, as schematically represented in Figs. 3a and 4, respectively, for a six-storey shear-type structure) and are sized so that each damping coefficient is proportional to the corresponding storey mass (m_i);
- *SPD system*: dampers are placed so that they connect adjacent storeys (Fig. 3b), and are sized so that each damping coefficient is proportional to the total lateral stiffness of the vertical elements that connect the same two storeys (k_i).

This is a new observation which opens up new possibilities of facing in an innovative, across-the-board manner the problem of optimal damper insertion in shear-type structures, by taking into consideration damper placements other that the traditional interstorey one. As far as the actual applicability of MPD systems in real building structures is concerned (SPD systems can be obtained placing dampers between adjacent storeys, as per the common damper setup), the interested reader is referred to Ref. [17–20]. In these works, the authors face this issue with specifically dedicated sections

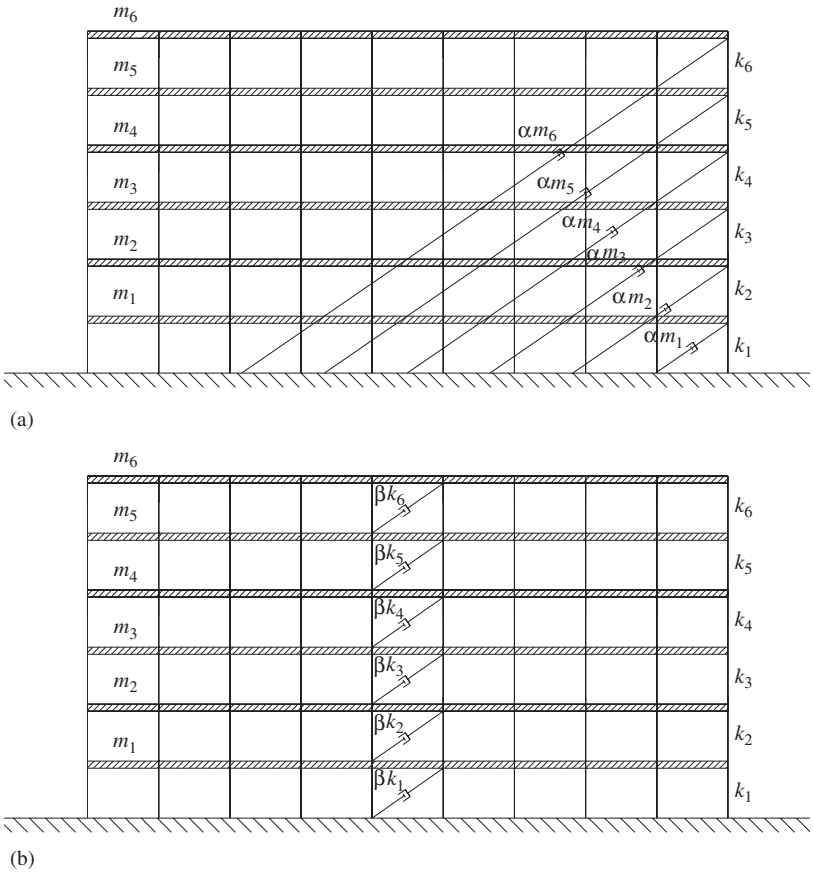

Fig. 3. Six-storey shear-type structure equipped with (a) MPD system (using the ground as fixed point) and (b) SPD system.

and identify two ways of implementing MPD systems: (i) using long buckling-resistant dampers capable of connecting to the ground floors up to three storey high (which are already available in the market place [10–14]) and (ii) placing the dampers between the floors and a very stiff vertical lateral-resisting element (e.g., concrete core or adjacent structure), as per Fig. 4, as also suggested (although without recognising the connection with the MPD system) by other authors [21–23].

4. The shear-type structures considered

The analytical results developed in the forthcoming sections refer to shear-type buildings having the following characteristics:

- total number of storeys $N \geqslant 2$;
- horizontal stiffness of the vertical elements connecting adjacent floors which does not vary along the height of the structure, i.e. $ki = k, \forall i$ (this hypothesis is realistic for steel frame

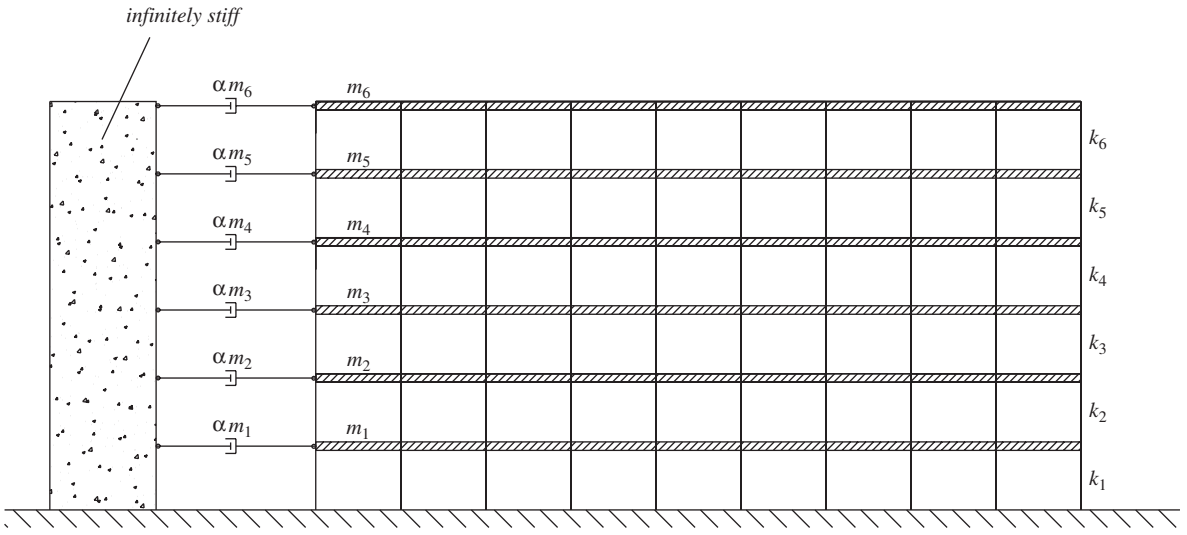

Fig. 4. Six-storey shear-type structure equipped with MPD system (using a infinitely stiff vertical lateral-resisting element as fixed point).

structures and may be assumed as correct for reinforced-concrete frame structures up to four–five storeys high);

- storey mass which does not vary along the height of the structure, i.e. $m_i = m, \forall i$ (this hypothesis is realistic for most frame structures).

These stiffness and mass values allow to define the following reference circular frequency:

$$\omega_0 = \sqrt{\frac{k}{m}}.$$

Under the above hypotheses, the mass and the stiffness matrices become

$$\mathbf{M}_N = m \underset{N\times N}{\begin{bmatrix} 1 & 0 & \ldots & & & \ldots & 0 \\ 0 & 1 & 0 & \ldots & & & \ldots \\ \ldots & 0 & \ldots & & & & \\ & & & & & & \\ & & & & \ldots & & \ldots \\ \ldots & & & & & 1 & 0 \\ 0 & \ldots & & & \ldots & 0 & 1 \end{bmatrix}}, \tag{10}$$

$$\mathbf{K}_N = k \underbrace{\begin{bmatrix} 2 & -1 & 0 & \dots & & & 0 \\ -1 & 2 & -1 & 0 & \dots & & \dots \\ 0 & -1 & 2 & \dots & & & \\ \dots & & \dots & \dots & & & \\ & & & & \dots & \dots & 0 \\ \dots & & & & \dots & 2 & -1 \\ 0 & \dots & & & & -1 & 1 \end{bmatrix}}_{N \times N}. \tag{11}$$

Here and in the following, the subscript $N \times N$ indicates the matrix size.

5. A constraint upon the total size of the damper systems

In order to make meaningful comparisons of the dissipative performances offered by different damper systems, it is necessary to introduce a constraint upon their total size. The total size (roughly representative of the cost of the damping systems), c_{tot}, of a generic damper system made up of M added viscous dampers is defined herein as the sum of the damping coefficients, c_j, of all M viscous dampers, as expressed by

$$\sum_{j=1}^{M} c_j = c_{\text{tot}}. \tag{12}$$

When various damper systems are compared, the equal "total size" constraint implies that all systems must have the same value, $\bar{c}$, of the total size, c_{tot}.

For the class of shear-type structures considered in this paper, imposing the equal "total size" constraint to the MPD and the SPD systems leads to the following results (note that, for N-storey shear-type structures, the MPD and the SPD systems are characterised by $M = N$):

- the α and β parameters assume the following specific values $\bar{\alpha}$ and $\bar{\beta}$:

$$\bar{\alpha} = \frac{\bar{c}}{Nm} = \frac{c_0}{m} \quad \text{for the MPD system,} \tag{13}$$

$$\bar{\beta} = \frac{\bar{c}}{Nk} = \frac{c_0}{k} \quad \text{for the SPD system} \tag{14}$$

  with $c_0 = \frac{\bar{c}}{N}$;
- the MPD and the SPD systems are made up of N equally sized dampers (each one characterised by $c0$). This is obtained firstly from substitution in Eq. (8) of the values $\bar{\alpha}$ and $\mathbf{M}$ given by Eqs. (13) and (10), respectively, and from substitution in Eq. (9) of the values $\bar{\beta}$ and $\mathbf{K}$ given by Eqs. (14) and (11), respectively, and secondly from comparison of the matrices of Eqs. (8) and (9) thus obtained with their physical counterparts given by Figs. 3a and b.

Note that Eqs. (13) and (14) lead to the following relationship between the $\bar{\alpha}$ and $\bar{\beta}$ values that guarantees the satisfaction of the equal "total size" constraint, independently of $\bar{c}$:

$$\bar{\alpha} = \bar{\beta}\omega_0^2. \tag{15}$$

For the class of shear-type structures considered in this paper, imposing the equal "total size" constraint to a generic Rayleigh damping system leads to the identification of a class of Rayleigh damping systems characterised by the following specific values $\bar{\alpha}^R$ and $\bar{\beta}^R$ of the α and β parameters:

$$\bar{\alpha}^R = \bar{\alpha}(1-\gamma) \quad \text{and} \quad \bar{\beta}^R = \bar{\beta}\gamma, \tag{16}$$

where γ is a dimensionless parameter with values ranging between 0 and 1, that identifies each specific Rayleigh system within the class defined above. Note that $\gamma = 0$ identifies the MPD system, whilst $\gamma = 1$ identifies the SPD system.

6. Modal damping ratios of structures equipped with MPD and SPD systems

For classically damped multi-degree-of-freedom (MDOF) systems, it is possible to define a damping ratio for each mode of vibration [15,16]. For Rayleigh-damped structures, it is well known that the ith modal damping ratio, ξ_i^R, expressed according to the notation of Eq. (7), is given by

$$\xi_i^R(\omega_i) = \frac{\alpha}{2\omega_i} + \frac{\beta\omega_i}{2}, \tag{17}$$

where ω_i is the ith modal (undamped) circular frequency of the MDOF system.

Specialising Eq. (17) to structures equipped with MPD system only, leads to

$$\xi_i^{\mathrm{MPD}}(\omega_i) = \frac{\alpha}{2\omega_i}. \tag{18}$$

Similarly, for structures equipped with SPD system only

$$\xi_i^{\mathrm{SPD}}(\omega_i) = \frac{\beta\omega_i}{2}. \tag{19}$$

The above equations clearly show that the MPD and the SPD systems, in addition to being physically separated as given in Section 3, display completely different damping properties:

- structures equipped with MPD systems are characterised by a modal damping ratio which progressively (hyperbolically) decreases as the modal frequency gets higher and higher;
- structures equipped with SPD systems are characterised by a modal damping ratio which linearly increases as the modal frequency gets higher and higher.

For the structures here considered (Section 4), imposing to Eqs. (18), (19) and (17) the equal "total size" constraint in the form of Eqs. (15) and (16) leads to

$$\xi_i^{\mathrm{MPD}} = \frac{\bar{\alpha}}{2\omega_i} = \frac{\bar{\alpha}}{2\omega_0}\left(\frac{\omega_0}{\omega_i}\right) = \frac{\xi_0}{\mathbf{\Omega}_i}, \tag{20}$$

$$\xi_i^{\mathrm{SPD}} = \frac{\bar{\beta}\omega_i}{2} = \frac{\bar{\alpha}\omega_i}{2\omega_0^2} = \frac{\bar{\alpha}}{2\omega_0}\left(\frac{\omega_i}{\omega_0}\right) = \xi_0 \boldsymbol{\Omega}_i, \tag{21}$$

$$\begin{aligned} \xi_i^R &= \frac{\bar{\alpha}^R}{2\omega_i} + \frac{\bar{\beta}^R \omega_i}{2} \\ &= \frac{\bar{\alpha}}{2\omega_i}(1-\gamma) + \frac{\bar{\beta}\omega_i}{2}\gamma \\ &= \xi_i^{\mathrm{MPD}}(1-\gamma) + \xi_i^{\mathrm{SPD}}\gamma \\ &= \xi_i^{\mathrm{MPD}} - \gamma\left(\xi_i^{\mathrm{MPD}} - \xi_i^{\mathrm{SPD}}\right), \end{aligned} \tag{22}$$

where

- $\Omega_i = \omega_i/\omega_0$ is the ith normalised circular frequency (with respect to the reference circular frequency $\omega 0$);
- $\xi_0 = \bar{\alpha}/(2\omega_0) = \bar{\beta}/(2\omega_0) = \bar{c}/(2N\sqrt{km}) = c_0/(2\sqrt{km})$ is a reference damping ratio that only depends on the characteristics of the structure (k, m and N) and the total size ($\bar{c}$) of the damping system. It is worth pointing out that ξ_0 corresponds to the damping ratio of a single-storey shear-type structure with lateral stiffness equal to k, floor mass equal to m and damper coefficient equal to c_0.

From Eqs. (20) and (21), it can be deduced that

$$\frac{\xi_i^{\mathrm{SPD}}}{\xi_j^{\mathrm{MPD}}} = \Omega_i \Omega_j \tag{23}$$

and

$$\frac{\xi_i^{\mathrm{SPD}}}{\xi_i^{\mathrm{MPD}}} = \Omega_i^2. \tag{24}$$

It is clear that:

- if $\Omega_i = 1$, then $\xi_i^{\mathrm{MPD}} = \xi_0 = \xi_i^{\mathrm{SPD}}$;
- if $\Omega_i < 1$, then $\xi_i^{\mathrm{MPD}} > \xi_0 > \xi_i^{\mathrm{SPD}}$;
- if $\Omega_i > 1$, then $\xi_i^{\mathrm{MPD}} < \xi_0 < \xi_i^{\mathrm{SPD}}$.

Specialising Eq. (24) for $i = 1$ leads to

$$\frac{\xi_1^{\mathrm{SPD}}}{\xi_1^{\mathrm{MPD}}} = \Omega_1^2. \tag{25}$$

From Eq. (25) it is clear that, if, for a given structure among those here considered, Ω_1 is smaller than unity (as will be demonstrated in the following sections), then the insertion into the structure of an MPD system leads to a damping ratio of the fundamental mode of vibration which is larger than that given by the insertion into the structure of an SPD system.

Also from Eq. (22) it is clear that, if, for a given structure among those here considered, Ω_1 is smaller than unity, then the insertion into the structure of an MPD system leads to a damping ratio of the fundamental mode of vibration which is larger than that given by the insertion into the structure of any Rayleigh damping system.

Note that the value of Ω_1 is a physical property of the system and, therefore, the above considerations are independent from the type of the excitation. Nonetheless, identifying a damping system which leads to the largest damping ratio in the first mode of vibration is of particular interest for building structures under base excitation (such as earthquake inputs), given that their dynamic response is greatly influenced by the first mode of vibration.

7. On the eigenproblem leading to the determination of Ω_i

For the generic N-storey shear-type structure here considered, the N modal (undamped) circular frequencies, ω_i, of the system are given by the square roots of the eigenvalues, λ_i, ($\omega_i = \sqrt{\lambda_i}$) of the following eigenproblem:

$$\mathbf{K}_N - \lambda \mathbf{M}_N = \mathbf{0}, \tag{26}$$

where $\mathbf{0}$ is a N-dimensional vector of all zero values.

Defining the following numerical matrix:

$$\mathbf{A}_N = \frac{1}{\omega_0^2}\mathbf{K}_N\mathbf{M}_N^{-1} = \underset{N\times N}{\begin{bmatrix} 2 & -1 & 0 & ... & & & 0 \\ -1 & 2 & -1 & 0 & ... & & 0 \\ 0 & -1 & 2 & ... & ... & & ... \\ ... & 0 & ... & ... & & & ... \\ & & ... & & ... & -1 & 0 \\ & & & & -1 & 2 & -1 \\ 0 & ... & & ... & 0 & -1 & 1 \end{bmatrix}} \tag{27}$$

the eigenvalue problem of Eq. (26) can be expressed as follows:

$$\mathbf{A}_N - \Lambda \mathbf{I}_N = \mathbf{0}, \tag{28}$$

where

- $\mathbf{I}_N$ is the identity matrix of order N;
- the eigenvalues Λ_i of Eq. (28) are related to the eigenvalues λ_i of Eq. (26) as follows:

$$\Lambda_i = \frac{\lambda_i}{\omega_0^2} = \frac{\omega_i^2}{\omega_0^2} = \Omega_i^2. \tag{29}$$

By definition, Λ_i are the N zeros (roots) [24–28] of the characteristic polynomial $p_N(\Lambda)$ of the numerical matrix $\mathbf{A}_N$, as given by

$$p_N(\Lambda) = \det(\mathbf{A}_N - \Lambda \mathbf{I}_N). \tag{30}$$

Note that Λ_i: (a) are independent of k and m, and (b) provide direct information on the modal damping ratios of the structures equipped with MPD and SPD systems as given by Eqs. (24) and (29).

$p_N(\Lambda)$ can also be expressed in the general form

$$p_N(\Lambda) = a_0 + a_1\Lambda + \cdots + a_{N-1}\Lambda^{N-1} + a_N\Lambda^N, \tag{31}$$

where a_0, a_1, …, a_i, …, a_{N-1} and a_N are constant coefficients.

The properties of matrix $\mathbf{A}_N$ allow to show that (as demonstrated in Appendices A.2–A.5) a_0, a_1, a_N and a_{N-1} have the following values:

$$a_0 = 1, \tag{32.1}$$

$$a_1 = -\frac{N(N+1)}{2}, \tag{32.2}$$

$$a_N = (-1)^N, \tag{32.3}$$

$$a_{N-1} = (-1)^{N-1}(2N-1). \tag{32.4}$$

In the following, in order to distinguish between the coefficients of polynomials of different degree N, the notation "$a_{i,N}$" will be used, which indicates the multiplicative coefficient of the term of degree i of the characteristic polynomial of the $N \times N$ matrix $\mathbf{A}_N$. Similarly, "$\Lambda_{i,N}$" or "$\Lambda_i(N)$" will represent the ith eigenvalue of the $N \times N$ matrix $\mathbf{A}_N$.

8. On the first modal damping ratios

In this section, a detailed analysis of the values assumed by $\Lambda_{1,N}$ will be performed. Thanks to Eqs. (20), (21), (25) and (29), the results obtained for $\Lambda_{1,N}$ will allow a number of considerations regarding the relative values of ξ_1^{MPD} and ξ_1^{SPD} to be drawn.

Given that the numerical matrix $\mathbf{A}_N$ of Eq. (27) is real and symmetric, all eigenvalues Λ_i are real [24–28]. Furthermore, being $\mathbf{A}_N$ positive definite (as it is the product of two positive definite matrices multiplied by a positive real scalar), all eigenvalues Λ_i are strictly positive [26–28]. Therefore, by numbering the eigenvalues Λ_i from the smallest to the largest, it is possible to write:

$$0 < \Lambda_1 \leqslant \Lambda_2 \leqslant \cdots \leqslant \Lambda_N. \tag{33}$$

8.1. On the values of Λ_1

From mathematics [29] it is known that, for the polynomial of degree $N \geqslant 1$:

$$p_N(x) = b_0 + b_1 x + \cdots + b_{N-1}x^{N-1} + b_N x^N, \tag{34}$$

the following relationships exist between the N zeros x_i and the $N+1$ complex coefficients b_0, …, b_{N-1}, b_N:

$$x_1 + x_2 + \ldots + x_N = \sum_{i=1}^{N} x_i = (-1)^1 \frac{b_{N-1}}{b_N} \tag{35.1}$$

$$x_1x_2 + x_1x_3 + \ldots + x_{N-1}x_N = \sum_{i=1}^{N}\sum_{j=i+1}^{N} x_ix_j = (-1)^2\frac{b_{N-2}}{b_N}$$

$$\ldots \tag{35.2}$$

$$x_1x_2\ldots x_{N-1} + x_1x_2\ldots x_{N-2}x_N + \ldots + x_2x_3\ldots x_N = (-1)^{N-1}\frac{b_1}{b_N} \tag{35.N-1}$$

$$x_1x_2\ldots x_N = \prod_{i=1}^{N} x_i = (-1)^N\frac{b_0}{b_N}. \tag{35.N}$$

Specialising the above relationships for the polynomial of Eq. (30) (substitution of Eqs. (31) and (32) into Eqs. (35.1) and (35.N)) leads to:

$$\Lambda_1 + \Lambda_2 + \ldots + \Lambda_N = -\frac{a_{N-1}}{a_N} = -\frac{(-1)^{N-1}(2N-1)}{(-1)^N} = 2N-1 \tag{36}$$

$$\Lambda_1\Lambda_2\ldots\Lambda_N = (-1)^N\frac{a_0}{a_N} = (-1)^N\frac{1}{(-1)^N} = 1. \tag{37}$$

From Eq. (37) it results that:

(a) either all Λ_i are equal to unity,
(b) or at least one Λ_i is strictly smaller than unity and at least one Λ_i is strictly larger than unity.

However, only case (b) is possible, because, if case (a) were true, then:

$$\Lambda_1 + \Lambda_2 + \ldots + \Lambda_N = N \tag{38}$$

which does not satisfy Eq. (36), given that

$$N < 2N-1 \quad \text{for} \quad N \geqslant 2 \text{ here considered.} \tag{39}$$

Therefore

$$\Lambda_1 < 1, \tag{40}$$

$$\Lambda_N > 1. \tag{41}$$

Eqs. (25), (29) and (40) lead to the fundamental result

$$\frac{\xi_1^{\mathrm{SPD}}}{\xi_1^{\mathrm{MPD}}} = \Omega_1^2 = \Lambda_1 < 1. \tag{42}$$

From basic physics and mathematics, it is thus shown that, for the class of shear-type structures characterised by constant values of lateral stiffness, k, and storey mass, m, and by a total number of storey $N \geqslant 2$, the MPD system provides the structure with a first modal damping ratio which is larger than that provided by the SPD system and any Rayleigh damping system (from Eqs. (22) and (42)) that satisfy the equal "total size" constraint.

8.2. An upper bound for $\Lambda_{1,N}$

In this section the attention is focused on the values of $\Lambda_{1,N}$ (which belongs to the interval (0,1), as given above) with the aim of obtaining an upper bound as a function of N.

Let us define:

$$f_N(\Lambda) = \frac{p_{N-2}(\Lambda)}{p_{N-1}(\Lambda)}. \tag{43}$$

Given that (as will be demonstrated in Appendix A.1):

$$p_N(\Lambda) = (2-\Lambda)p_{N-1}(\Lambda) - p_{N-2}(\Lambda) \tag{44}$$

the zeros ($\Lambda_{i,N}$) of $p_N(\Lambda) = 0$ correspond to the intersections between:

- the straight line $g(\Lambda) = 2 - \Lambda$,
- and the function $f_N(\Lambda)$

and therefore $\Lambda_{1,N}$ corresponds to the first intersection which occurs for $\Lambda \in (0,1)$.

As illustrative examples, see Figs. 5a and b for graphical representations of the above curves within the interval $\Lambda \in (0,1)$.

Eq. (43) gives that $f_N(\Lambda)$ has vertical asymptotes in correspondence of the zeros ($\Lambda_{i,N-1}$) of $p_{N-1}(\Lambda)$.

Note that $g(\Lambda)$ is monotonically decreasing.

Also, $f_N(\Lambda)$ is increasing, due to the fact that (as will be demonstrated in Appendix A.6) the first derivative of $f_N(\Lambda)$ is always strictly positive.

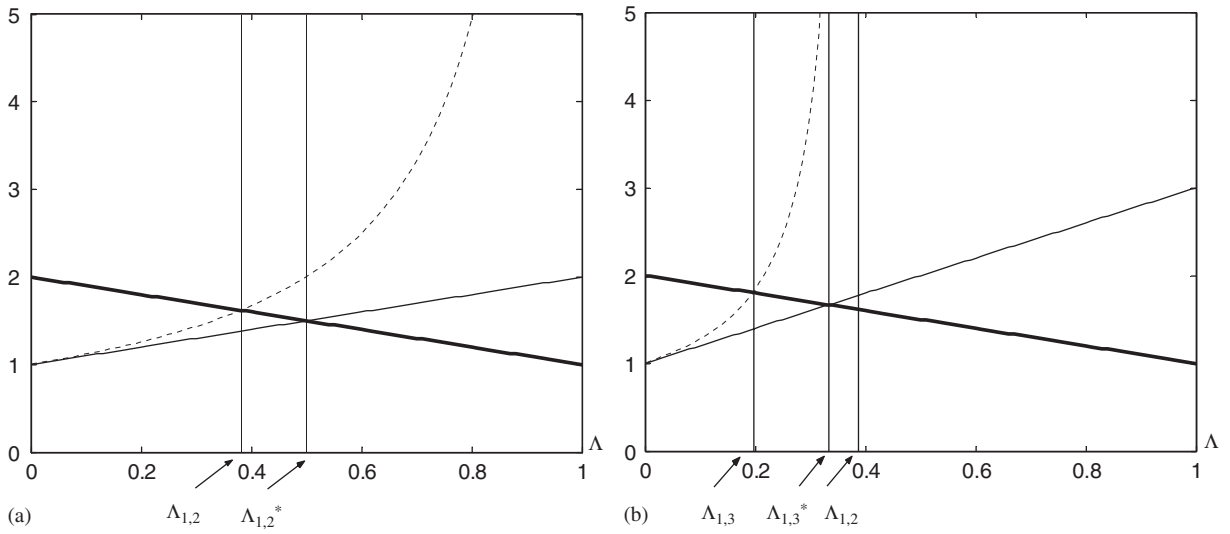

Fig. 5. $g(\Lambda)$ (black thick continuous line), $f_N(\Lambda)$ (black dashed line), and $f_N^*(\Lambda)$ (black thin continuous line) for (a) $N = 2$ and (b) $N = 3$.

Given the above properties and the fact that:

- $g(0) = 2$;
- $f_N(0) = \frac{p_{N-2}(0)}{p_{N-1}(0)} = \frac{a_{0,N-2}}{a_{0,N-1}} = 1$;
- $\Lambda = \Lambda_{1,N-1}$ is the first vertical asymptote of $f_N(\Lambda)$;

from basic geometrical and analytical considerations, it follows that $g(\Lambda)$ and $f_N(\Lambda)$ intersect between zero and $\Lambda_{1,N-1}$ [29], i.e.

$$\Lambda_{1,N} < \Lambda_{1,N-1}. \tag{45}$$

Furthermore, given that (as will be demonstrated in Appendix A.7) the second derivative of $f_N(\Lambda)$ is strictly positive for $\Lambda \in (0,\Lambda_{1,N-1})$, $f_N(\Lambda)$ is increasing with an up curvature, between zero and $\Lambda_{1,N-1}$. It follows that the intersection $\Lambda^*_{1,N}$ between $g(\Lambda)$ and the tangent, $f^*_N(\Lambda)$, to $f_N(\Lambda)$ at $\Lambda = 0$ is larger than $\Lambda_{1,N}$ [29], i.e.

$$\Lambda_{1,N} < \Lambda^*_{1,N}. \tag{46}$$

The tangent $f^*_N(\Lambda)$ has the following expression:

$$f^*_N(\Lambda) = f'_N(0)\Lambda + f_N(0) \tag{47}$$

and, computing its intersection with $g(\Lambda)$, leads to

$$\Lambda^*_{1,N} = \frac{2 - f_N(0)}{1 + f'_N(0)}. \tag{48}$$

Given that $f_N(0) = 1$ and $f'_N(0) = N - 1$ (as will be shown in Appendix A.8)

$$\Lambda^*_{1,N} = \frac{1}{N} \tag{49}$$

and

$$\Lambda_{1,N} < \frac{1}{N} \quad \forall N. \tag{50}$$

8.3. A close approximation for $\Lambda_{1,N}$

From Eq. (50) we observe that, as N increases, the first root $\Lambda_{1,N}$ of the characteristic polynomial $p_N(\Lambda)$ of Eq. (30) tends to zero. Therefore, within the interval $\Lambda \in (0,\Lambda_{1,N})$, $p_N(\Lambda)$ can be effectively approximated neglecting the terms of degree higher than one, i.e.

$$p_N(\Lambda) \cong \bar{p}_N(\Lambda) = a_0 + a_1\Lambda \quad \text{for} \quad \Lambda \in \left(0, \Lambda_{1,N}\right). \tag{51}$$

In accordance to the above approximation, an estimation $\bar{\Lambda}_{1,N}$ of $\Lambda_{1,N}$ can be obtained imposing $\bar{p}_N(\Lambda) = 0$, which leads to

$$\bar{\Lambda}_{1,N} = \frac{-a_0}{a_1} = \frac{2}{N(N+1)} \cong \Lambda_{1,N}. \tag{52}$$

This approximation becomes more and more precise, as N increases, and it is numerically seen to be very effective for $N \geqslant 6$ (see also the applicative example of Section 11).

8.4. ξ_1^{MPD}, ξ_1^{SPD} and their ratio as functions of N

As an illustrative example, Fig. 6 shows $\Lambda_1(N)$ for N varying from 2 to 20, as obtained for the shear-type structures here analysed. The figure also shows the curves $y = 1/N$ and $y = 2/(N^2 + N)$ which, as demonstrated before, respectively represent an upper bound and a close approximation of $\Lambda_1(N)$.

The properties of $\Lambda_1(N)$ given by Eqs. (50) and (52), thanks to Eqs. (20), (21), (25) and (29), lead directly to the following considerations upon ξ_1^{MPD}, ξ_1^{SPD} and ξ_1^{SPD}/ξ_1^{MPD}:

- $\xi_1^{MPD} > \xi_0\sqrt{N}$,
- $\xi_1^{SPD} < \frac{\xi_0}{\sqrt{N}}$,
- $\frac{\xi_1^{SPD}}{\xi_1^{MPD}} < \frac{1}{N}$,
- $\xi_1^{MPD} \cong \xi_0\sqrt{\frac{N^2+N}{2}}$,
- $\xi_1^{SPD} \cong \xi_0\sqrt{\frac{2}{N^2+N}}$,
- $\frac{\xi_1^{SPD}}{\xi_1^{MPD}} \cong \frac{2}{N^2+N}$.

Note that, releasing the equal "total size" constraint, with reference to a targeted damping ratio ξ_t and its corresponding damping coefficient $c_t = 2\xi_t\sqrt{km}$, imposing that $\xi_1^{MPD} = \xi_1^{SPD} = \xi_t$ leads to

$$c^{MPD} = c_t\Omega_1 = c_t\sqrt{\Lambda_1}, \tag{53}$$

$$c^{SPD} = \frac{c_t}{\Omega_1} = \frac{c_t}{\sqrt{\Lambda_1}}, \tag{54}$$

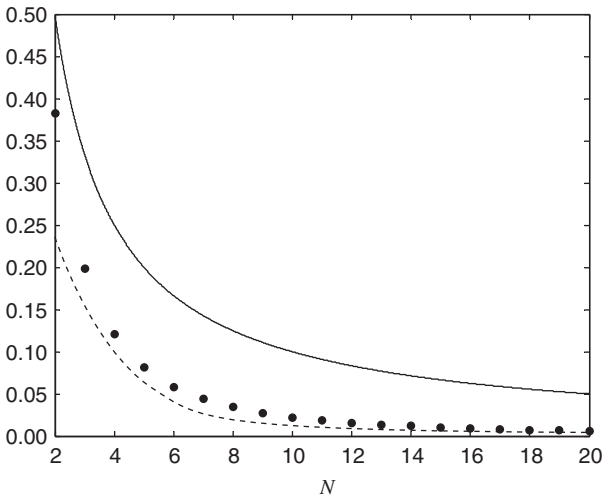

Fig. 6. $\Lambda_1(N)$ (black dots), $y = 1/N$ (continuous line) and $y = 2/(N^2 + N)$ (dashed line) for N varying from 2 to 20.

where c^{MPD} and c^{SPD} represent the damping coefficient of each viscous damper of the MPD and SPD system, respectively. Eqs. (50), (53) and (54) give that

- in order to obtain, for a N-storey structure equipped with the MPD system, a first modal damping ratio at least as large as the targeted damping ratio ξ_t, it is sufficient to place at every storey a damper of size $c_t/\sqrt{N}$;
- for a N-storey structure equipped with the SPD system, even the placement at every storey of dampers of size $c_t/\sqrt{N}$ leads to a first modal damping ratio smaller than ξ_t.

9. On the damping ratios of higher modes

Let p be the number of roots of the characteristic polynomial of Eq. (30) that are less or equal than unity. In general

$$1 \leqslant p \leqslant N-1. \tag{55}$$

If $p=1$, i.e. $\Lambda_1<1$, $\Lambda_2>1$, …, $\Lambda_N>1$, from Eq. (37), it is possible to write

$$1=\Lambda_1\Lambda_2\ldots\Lambda_{N-1}\Lambda_N>\Lambda_1\cdot 1\ldots 1\cdot\Lambda_N=\Lambda_1\Lambda_N. \tag{56}$$

It follows that

$$\frac{\xi_N^{\mathrm{SPD}}}{\xi_1^{\mathrm{MPD}}}=\Omega_1\Omega_N=\sqrt{\Lambda_1\Lambda_N}<1. \tag{57}$$

Therefore, from Eqs. (21), (29), (33) and (57)

$$\xi_1^{\mathrm{MPD}}>\xi_N^{\mathrm{SPD}}>\xi_{N-1}^{\mathrm{SPD}}>\cdots>\xi_1^{\mathrm{SPD}}. \tag{58}$$

On the other hand, if $p>1$, i.e. $\Lambda_1<1$, …, $\Lambda_p\leqslant 1$, $\Lambda_{p+1}>1$, …, $\Lambda_N>1$, from Eq. (37), it is possible to write

$$\begin{aligned}1&=\Lambda_1\ldots\Lambda_p\,\Lambda_{p+1}\,\ldots\,\Lambda_{N-p}\,\Lambda_{N-p+1}\,\ldots\,\Lambda_N\\&>\Lambda_1\ldots\Lambda_1\,\Lambda_{p+1}\,\ldots\,\Lambda_{N-p}\,\Lambda_{N-p+1}\,\ldots\,\Lambda_{N-p+1}\\&>\Lambda_1^p\cdot 1\ldots 1\cdot\Lambda_{N-p+1}^p=\left(\Lambda_1\Lambda_{N-p+1}\right)^p\end{aligned} \tag{59}$$

It follows that

$$\frac{\xi_{N-p+1}^{\mathrm{SPD}}}{\xi_1^{\mathrm{MPD}}}=\Omega_1\Omega_{N-p+1}=\sqrt{\Lambda_1\Lambda_{N-p+1}}<1. \tag{60}$$

Therefore, from Eqs. (21), (29), (33) and (60)

$$\xi_1^{\mathrm{MPD}}>\xi_{N-p+1}^{\mathrm{SPD}}>\xi_{N-p}^{\mathrm{SPD}}>\cdots>\xi_1^{\mathrm{SPD}} \tag{61}$$

Moreover, it is also immediate that, for $i=1, 2, \ldots, p-1$:

$$\frac{\xi_i^{\mathrm{SPD}}}{\xi_i^{\mathrm{MPD}}}=\Omega_i^2=\Lambda_i<1 \tag{62}$$

and for $i = p$:

$$\frac{\xi_p^{\mathrm{SPD}}}{\xi_p^{\mathrm{MPD}}} = \Omega_p^2 = \Lambda_p \leqslant 1. \tag{63}$$

It is numerically seen that $p = \left[(N+2)/3\right]$ (where $[z]$ indicates the integer part of z) and therefore, for systems characterised by a large N, it results $p \cong N/3$, which gives that $\xi_i^{\mathrm{MPD}} > \xi_i^{\mathrm{SPD}}$ roughly for the first $N/3$ modes of vibration.

10. Other properties of modal damping ratios of MPD and SPD structures

A number of other considerations can be made regarding the modal damping ratios of structures equipped with MPD and SPD systems.

Taking into consideration the product of the ith modal damping ratios of MPD and SPD structures, from Eqs. (20) and (21), it can be immediately seen that

$$\xi_i^{\mathrm{MPD}} \xi_i^{\mathrm{SPD}} = \xi_0^2 = \text{constant}. \tag{64}$$

This equation underlines the opposite dissipative properties of MPD and SPD systems. In fact, if the ith modal damping ratio of the MPD structure is large, then the ith modal damping ratio of the SPD structure is small, and vice versa.

Taking into consideration the sum of the squares of all damping ratios of MPD and SPD structures, from Eqs. (20), (21), (29), (32) and (35), it can be seen that

$$\begin{aligned}
\frac{\sum_{i=1}^{N} \left(\xi_i^{\mathrm{MPD}}\right)^2}{\sum_{i=1}^{N} \left(\xi_i^{SPD}\right)^2} &= \frac{\frac{1}{\Lambda_1} + \frac{1}{\Lambda_2} + \cdots + \frac{1}{\Lambda_N}}{\Lambda_1 + \Lambda_2 + \cdots + \Lambda_N} \\
&= \frac{\left(\frac{\Lambda_2\Lambda_3\cdots\Lambda_N + \Lambda_1\Lambda_3\cdots\Lambda_N + \cdots + \Lambda_1\Lambda_2\cdots\Lambda_{N-1}}{\Lambda_1\Lambda_2\cdots\Lambda_N}\right)}{\Lambda_1 + \Lambda_2 + \cdots + \Lambda_N} \\
&= \frac{\left(\frac{(-1)^{N-1} a_1/a_N}{(-1)^N a_0/a_N}\right)}{(-1)^1 \frac{a_{N-1}}{a_N}} = \frac{a_1 a_N}{a_0 a_{N-1}} = \frac{-\frac{N(N+1)}{2}(-1)^N}{1(-1)^{N-1}(2N-1)} \\
&= \frac{N(N+1)}{2(2N-1)} = \frac{N^2+N}{4N-2}.
\end{aligned} \tag{65}$$

The geometrical sum of the damping ratios

$$\xi_{\mathrm{g.s.}} = \sqrt{\sum_{i=1}^{N} \xi_i^2} \tag{66}$$

can be reasonably assumed as performance index of the dissipative effects of the MPD and SPD systems. The ratio of the two geometrical sums as obtained for the MPD and SPD systems

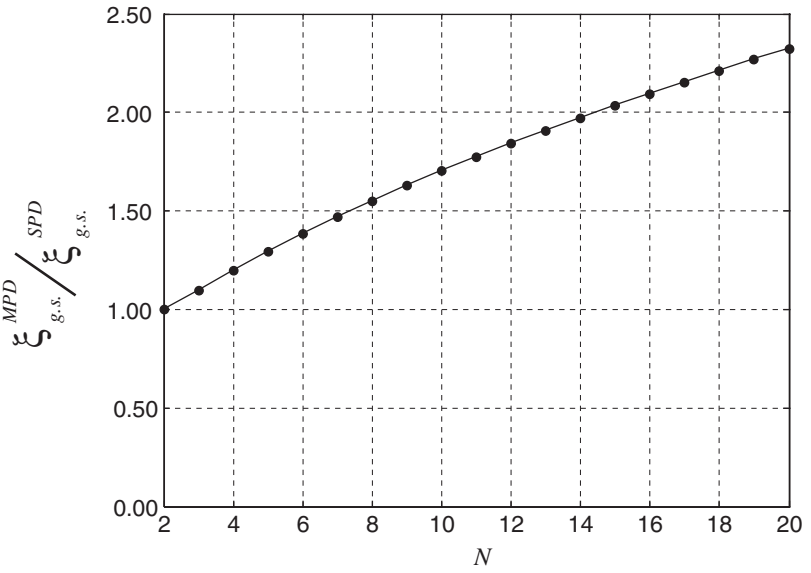

Fig. 7. $\xi_{\text{g.s.}}^{\text{MPD}} \Big/ \xi_{\text{g.s.}}^{\text{SPD}}$ as a function of N (N varying from 2 to 20).

(denoted as $\xi_{\text{g.s.}}^{\text{MPD}}$ and $\xi_{\text{g.s.}}^{\text{SPD}}$, respectively), thanks to Eq. (65), can be expressed as

$$\frac{\xi_{\text{g.s.}}^{\text{MPD}}}{\xi_{\text{g.s.}}^{\text{SPD}}} = \sqrt{\frac{N^2+N}{4N-2}} \tag{67}$$

which is larger than unity for $N>2$ and increases for increasing N, as illustrated in Fig. 7.

11. A numerical application to a shear-type structure subjected to seismic excitation

To provide an illustrative numerical example of the dissipative properties of the MPD and the SPD systems, this section reports the results regarding the dynamic response of a seven-storey structure subjected to seismic excitation.

11.1. The reference structure

The structure considered is the seven-storey shear-type structure represented in Fig. 8. This structure (as those described in Section 4 for which all the demonstrations of the previous sections were carried out) is characterised by a lateral stiffness k of the vertical elements connecting adjacent storeys and a floor mass m which do not vary along the height of the building. The specific values of k and m are respectively $k = 2.8 \times 10^8$ N/m and $m = 1.5 \times 10^5$ kg. The reference circular frequency ω_0 is equal to 43.20 rad/s. Interstorey height is equal to 3.3 m.

Table 1 gives the periods of vibration T_i, the normalised circular frequencies Ω_i and the eigenvalues Λ_i of the reference structure. Note that, for $N = 7$, p (number of roots $\Lambda_i \leqslant 1$) is equal to $\left[\frac{7+2}{3}\right] = 3$ ($\Lambda_1 = 0.044 < 1$, $\Lambda_2 = 0.382 < 1$, $\Lambda_3 = 1.000 \leqslant 1$).

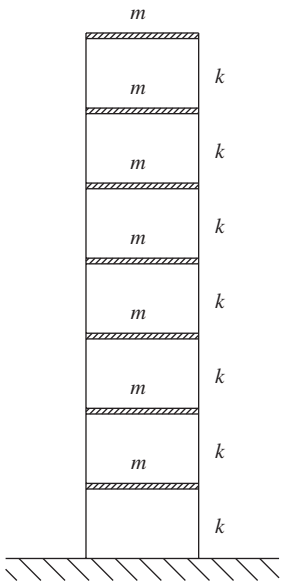

Fig. 8. Reference seven-storey shear-type structure.

Table 1
Periods of vibration T_i, normalised circular frequencies Ω_i and eigenvalues Λ_i of the reference structure

	Mode of vibration						
	1	2	3	4	5	6	7
T_i [s]	0.696	0.235	0.145	0.109	0.090	0.080	0.074
Ω_i [rad/s]	0.209	0.618	1.000	1.338	1.618	1.827	1.956
Λ_i	0.044	0.382	1.000	1.791	2.618	3.338	3.827

The structure is equipped with equal "total size" MPD and SPD systems made up of seven equally sized dampers, each one characterised by $c_j = c_0 = 2.5 \times 10^6\,\mathrm{N\,s/m}$, for which $\bar{c} = 1.75 \times 10^7\,\mathrm{N\,s/m}$. The reference damping ratio ξ_0 is equal to 0.192.

For illustrative examples of the dynamic behaviours of structures equipped with MPD and SPD systems having other physical characteristics (such as lateral stiffness of the vertical elements connecting adjacent storeys which varies along the building height) the interested reader is referred to other published research works of the authors [17–20, 30].

11.2. The modal damping ratios of the structure

This section illustrates some physical properties of the modal damping ratios which are independent from the type of excitation. Fig. 9 and Table 2 show the modal damping ratios of the reference structure equipped with the MPD and the SPD systems.

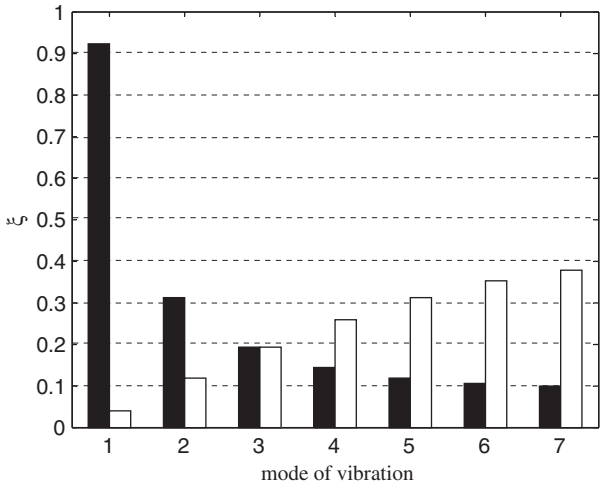

Fig. 9. Modal damping ratios for the seven-storey reference structure equipped with MPD system (black) and SPD system (white).

Table 2
Modal damping ratios of the MPD and the SPD structures

System	Mode of vibration						
	1	2	3	4	5	6	7
MPD	0.922	0.312	0.192	0.144	0.119	0.105	0.098
SPD	0.040	0.119	0.192	0.258	0.312	0.352	0.377

As anticipated by the theoretical findings of the previous sections:

- the modal damping ratio of the first mode of vibration of the MPD structure is far larger than that of the SPD structure ($\xi_1^{\mathrm{MPD}} = 0.922 > 0.040 = \xi_1^{\mathrm{SPD}}$),
- $\xi_2^{\mathrm{MPD}} = 0.312 > 0.119 = \xi_2^{\mathrm{SPD}}$, as anticipated by Eq. (62),
- $\xi_3^{\mathrm{MPD}} = 0.192 \geqslant 0.192 = \xi_3^{\mathrm{SPD}}$, as anticipated by Eq. (63) and by $p = 3$ and $\Lambda_3 = 1$,
- $\xi_i^{\mathrm{MPD}} < \xi_i^{\mathrm{SPD}}$, for $i = 4, 5, 6, 7$.

As per the results of Section 8.4:

- $\xi_1^{\mathrm{MPD}} = 0.922 > 0.508 = 0.192\sqrt{7} = \xi_0\sqrt{N}$,
- $\xi_1^{\mathrm{SPD}} = 0.040 < 0.073 = \frac{0.192}{\sqrt{7}} = \frac{\xi_0}{\sqrt{N}}$,
- $\frac{\xi_1^{\mathrm{SPD}}}{\xi_1^{\mathrm{MPD}}} = \frac{0.040}{0.922} = 0.043 < 0.143 = \frac{1}{7} = \frac{1}{N}$,
- $\xi_1^{\mathrm{MPD}} = 0.922 \cong 1.016 = 0.192\sqrt{\frac{7^2+7}{2}} = \xi_0\sqrt{\frac{N^2+N}{2}}$,

- $\xi_1^{\mathrm{SPD}} = 0.040 \cong 0.036 = 0.192\sqrt{\frac{2}{7^2+7}} = \xi_0\sqrt{\frac{2}{N^2+N}}$,
- $\frac{\xi_1^{\mathrm{SPD}}}{\xi_1^{\mathrm{MPD}}} = \frac{0.040}{0.922} = 0.043 \cong 0.036 = \frac{2}{7^2+7} = \frac{2}{N^2+N}$.

As per the results of Section 9 (Eq. (60)):

- $\frac{\xi_5^{\mathrm{SPD}}}{\xi_1^{\mathrm{MPD}}} = \frac{0.312}{0.922} = 0.338 < 1$.

Also, the largest modal damping ratio of the SPD is substantially smaller than the largest damping ratio of the MPD system

- $\frac{(\xi^{\mathrm{SPD}})_{\max}}{(\xi^{\mathrm{MPD}})_{\max}} = \frac{\xi_7^{\mathrm{SPD}}}{\xi_1^{\mathrm{MPD}}} = \frac{0.377}{0.922} = 0.409 < 1$.

As per the results of Section 10:

- $\xi_1^{\mathrm{MPD}}\xi_1^{\mathrm{SPD}} = 0.922 \cdot 0.040 = 0.037 = 0.192^2 = \xi_0^2$,
- $\xi_2^{\mathrm{MPD}}\xi_2^{\mathrm{SPD}} = 0.312 \cdot 0.119 = 0.037 = 0.192^2 = \xi_0^2$,
- $\xi_3^{\mathrm{MPD}}\xi_3^{\mathrm{SPD}} = 0.192 \cdot 0.192 = 0.037 = 0.192^2 = \xi_0^2$,
- $\xi_4^{\mathrm{MPD}}\xi_4^{\mathrm{SPD}} = 0.144 \cdot 0.258 = 0.037 = 0.192^2 = \xi_0^2$,
- $\xi_5^{\mathrm{MPD}}\xi_5^{\mathrm{SPD}} = 0.119 \cdot 0.312 = 0.037 = 0.192^2 = \xi_0^2$,
- $\xi_6^{\mathrm{MPD}}\xi_6^{\mathrm{SPD}} = 0.105 \cdot 0.352 = 0.037 = 0.192^2 = \xi_0^2$,
- $\xi_7^{\mathrm{MPD}}\xi_7^{\mathrm{SPD}} = 0.098 \cdot 0.377 = 0.037 = 0.192^2 = \xi_0^2$,
- $$\frac{\xi_{\mathrm{g.s.}}^{\mathrm{MPD}}}{\xi_{\mathrm{g.s.}}^{\mathrm{SPD}}} = \frac{\sqrt{0.922^2 + 0.312^2 + 0.192^2 + 0.144^2 + 0.119^2 + 0.105^2 + 0.098^2}}{\sqrt{0.040^2 + 0.119^2 + 0.192^2 + 0.258^2 + 0.312^2 + 0.352^2 + 0.377^2}} = \frac{1.020}{0.695}$$
$$= 1.468 = \sqrt{\frac{7^2+7}{4 \cdot 7 - 2}} = \sqrt{\frac{N^2+N}{4N-2}}.$$

Also, the sum of all damping ratios (representative of a "global" damping, if all modes of vibration had the same importance in determining the overall system response) of the MPD system is larger than that of the SPD one:

- $\left(\xi^{\mathrm{MPD}}\right)_{\mathrm{tot}} = \sum_{i=1}^{7} \xi_i^{\mathrm{MPD}} = 0.922 + 0.312 + 0.192 + 0.144 + 0.119 + 0.105 + 0.098 = 1.892$,
- $\left(\xi^{\mathrm{SPD}}\right)_{\mathrm{tot}} = \sum_{i=1}^{7} \xi_i^{\mathrm{SPD}} = 0.040 + 0.119 + 0.192 + 0.258 + 0.312 + 0.352 + 0.377 = 1.650$.

11.3. The damping properties of the structure under base (earthquake) excitation

For the generic N-storey linear elastic shear-type frame structure of Fig. 1 subjected to a horizontal (earthquake) input acceleration $\ddot{u}_g(t)$, the equations of motions can be written, in time

domain, as follows [15,16]:

$$\mathbf{M}\ddot{\mathbf{u}}(t) + \mathbf{C}\dot{\mathbf{u}}(t) + \mathbf{K}\mathbf{u}(t) = -\mathbf{M}\cdot\mathbf{1}\cdot\ddot{u}_g(t), \tag{68}$$

where $\mathbf{1}$ is a column vector of order N with each element equal to unity (influence vector).

It is worth recalling that, for structures subjected to base excitation, the first modes of vibration are the most important ones in the determination of the global response of the structure.

With reference to the modal analysis, in order to identify the relative importance of the different modes of vibrations in the determination of the global response of the structure, it is a common practice to define the modal contribution factor, $\bar{r}_n$, (a measure of the contribution of the nth mode to a generic response quantity r) as follows [16]:

$$\bar{r}_n = \frac{r_n^{\mathrm{st}}}{r^{\mathrm{st}}}, \tag{69}$$

where

- rst is the static value of the response quantity r due to a set $\mathbf{s}$ of static forces applied to the structure; $\mathbf{s}$ being defined as $\mathbf{s} = \mathbf{M}\cdot\mathbf{1}$;
- $r_{\mathrm{n}}^{\mathrm{st}}$ (nth modal static response) is the static value of the response quantity r due to a set $\mathbf{s}_n$ of static forces applied to the structure; $\mathbf{s}_n$ being defined as $\mathbf{s}_n = \Gamma_n\mathbf{M}\boldsymbol{\phi}_n$;
- $\boldsymbol{\phi}_n$ is the eigenvector corresponding to the nth modal frequency of the system;
- $\Gamma_n = \frac{\boldsymbol{\phi}_n^{\mathrm{T}}\cdot\mathbf{M}\cdot\mathbf{1}}{\boldsymbol{\phi}_n^{\mathrm{T}}\cdot\mathbf{M}\cdot\boldsymbol{\phi}_n}$ is the modal participation factor.

The N modal contribution factors, $\bar{r}_n$ defined above, are characterised by the following three properties [16]:

- they are dimensionless;
- they are independent of how the modes $\boldsymbol{\phi}_n$ are normalised;
- their sum over all modes is unity (i.e. $\sum_{i=1}^{N}\bar{r}_n = 1$).

If base shear, V_b, is assumed as significant response quantity [16], the modal contribution factor, $\bar{r}_n$, becomes $\bar{V}_{bn}$, as given by

$$\bar{V}_{bn} = \frac{V_{bn}^{\mathrm{st}}}{V_b^{\mathrm{st}}} = \frac{M_n^*}{\sum_{n=1}^{N} M_n^*}, \tag{70}$$

where $M_n^* = \Gamma_n\sum_{j=1}^{N} m_j\phi_{jn}$ represents the nth base shear effective modal mass [16] (with ϕ_{jn} being the jth component of $\boldsymbol{\phi}_n$).

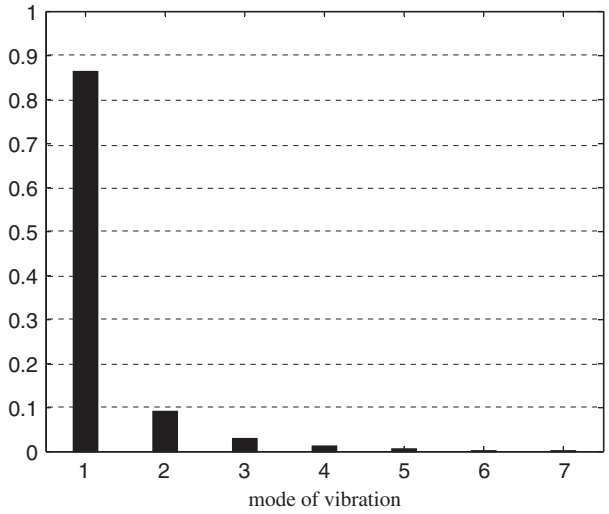

Fig. 10. Modal contribution factors, $\tilde{V}_{\mathrm{bn}}$, for the seven-storey reference structure.

Table 3
Modal contribution factors for the seven-storey reference structure

Mode of vibration						
1	2	3	4	5	6	7
0.8621	0.0902	0.0286	0.0118	0.0050	0.0019	0.0004

Fig. 10 and Table 3 show the modal contribution factors for the seven-storey reference structure. As it is the case for most of common shear-type structures, most of the contributions come from the first modes of vibration.

Note that, in the first mode of vibration which accounts for about 86% of the overall system response, the MPD system is characterised by a modal damping ratio of about 92%, while the SPD system is characterised by a modal damping ratio of about 4%. On the other hand, the 4th, 5th, 6th and 7th modes of vibration, for which the SPD system is characterised by modal damping ratios larger than those of the MPD system, together account for less than 2% of the overall system response.

This suggests that the seismic performances of the reference structure equipped with the MPD system are far superior than those of the same structure equipped with the SPD system.

11.4. The dynamic response of the structure under base (earthquake) excitation

Figs. 11, 12, 13 and 14 show respectively the profiles of peak floor displacements (PFD), peak floor velocities (PFV), peak floor accelerations (PFA) and peak interstorey drift angles (PIDA), as

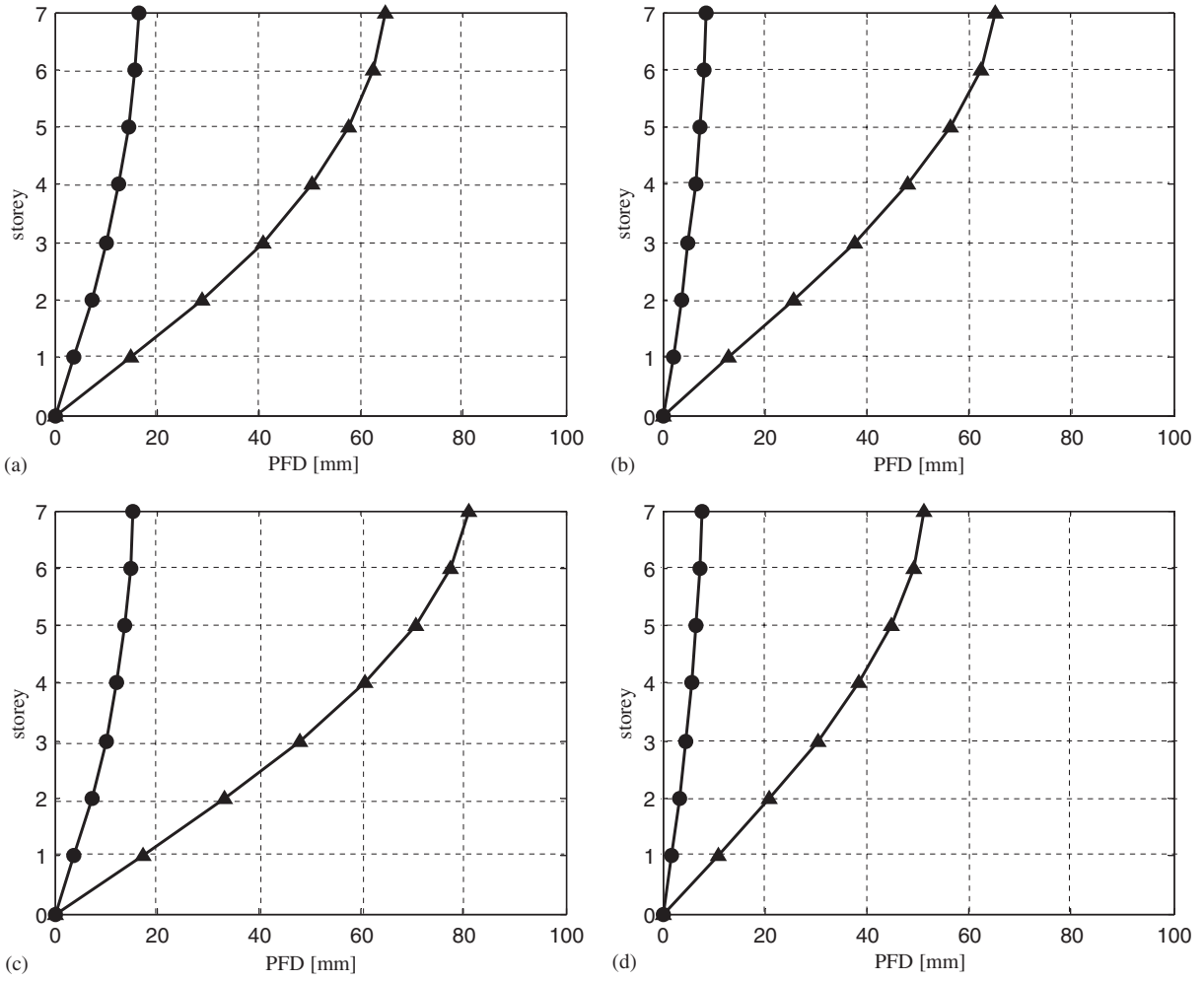

Fig. 11. Peak floor displacements (PFD) developed by the seven-storey reference structure equipped with MPD system (—●—) and SPD system (—▲—) under the earthquakes: (a) Imperial Valley, 1940 (El Centro record, NS component 270°, PGA = 0.215 g), (b) Kern County, 1952 (Taft Lincoln School record, EW component 21°, PGA = 0.156 g), (c) Kobe, 1995 (Kobe University record, NS component 90°, PGA = 0.310 g), (d) Northridge, 1994 (Camarillo record, EW component 180°, PGA = 0.125 g).

obtained using as $\ddot{u}_g(t)$ the following historically recorded earthquake ground motions: Imperial Valley, 1940 (El Centro record, NS component 270°, PGA = 0.215 g), Kern County, 1952 (Taft Lincoln School record, EW component 21°, PGA = 0.156 g), Kobe, 1995 (Kobe University record, NS component 90°, PGA = 0.310 g) and Northridge, 1994 (Camarillo record, EW component 180°, PGA = 0.125 g).

Notice how, in all cases considered, the response parameters of the structure equipped with the MPD system are always substantially smaller (−80%) than the corresponding ones of the structure equipped with the SPD system.

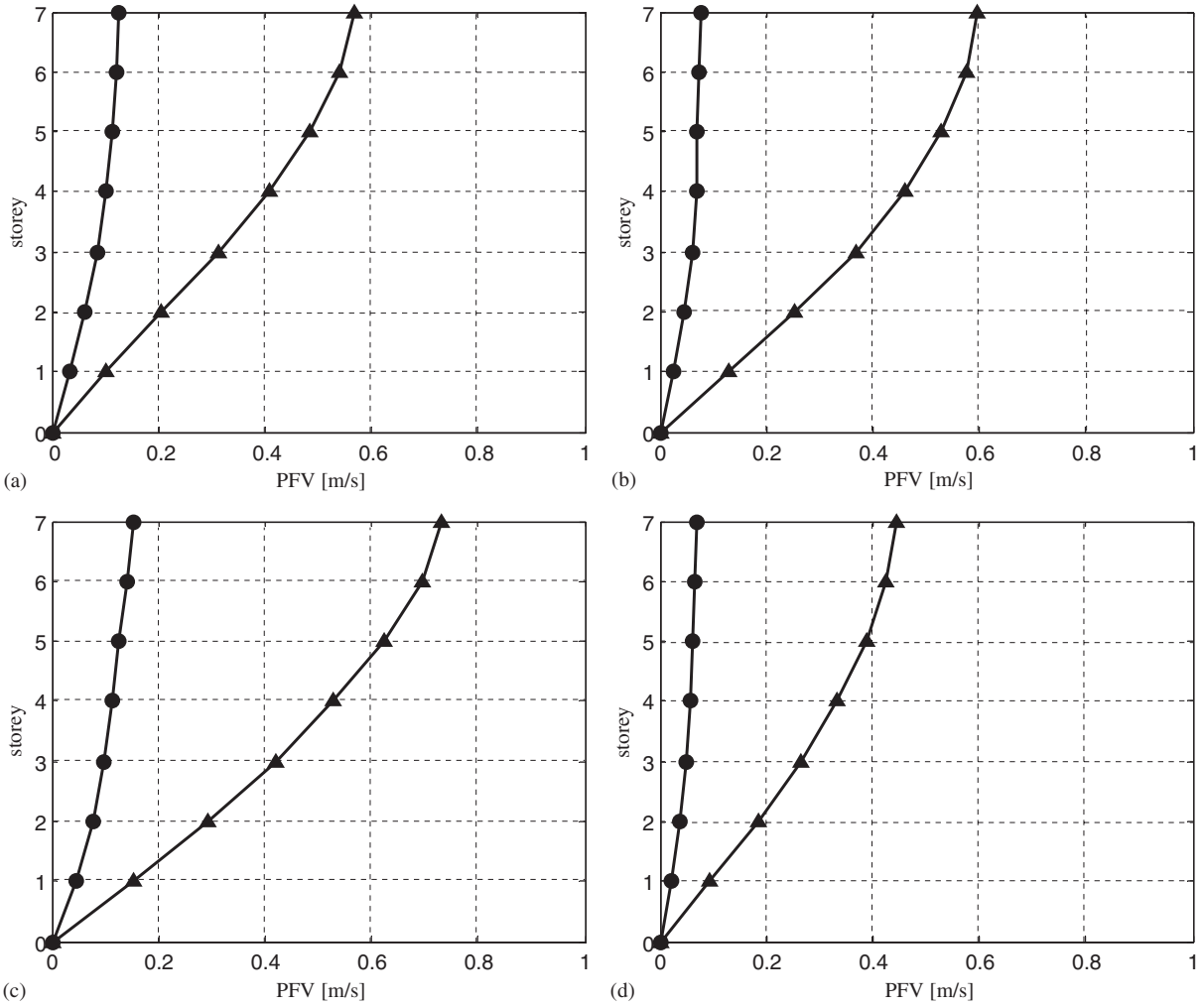

Fig. 12. Peak floor velocities (PFV) developed by the seven-storey reference structure equipped with MPD system (—●—) and SPD system (—▲—) under the earthquakes: (a) Imperial Valley, 1940 (El Centro record, NS component 270°, PGA = 0.215 g), (b) Kern County, 1952 (Taft Lincoln School record, EW component 21°, PGA = 0.156 g), (c) Kobe, 1995 (Kobe University record, NS component 90°, PGA = 0.310 g), (d) Northridge, 1994 (Camarillo record, EW component 180°, PGA = 0.125 g).

This is a numerical confirmation of the superior dissipative properties (with respect to earthquake dynamic inputs) of the MPD system with respect to the equal "total size" SPD system identified on the basis of the physical analyses developed in this paper.

In summary, the above results allow to propose the implementation of MPD systems in actual building structures (as per Figs. 3a and 4) in order to obtain reductions (up to about 80%) in the seismic response of shear-type buildings with respect to the equally sized (equal "total size" constraint) SPD systems commonly adopted in the seismic design of building structures.

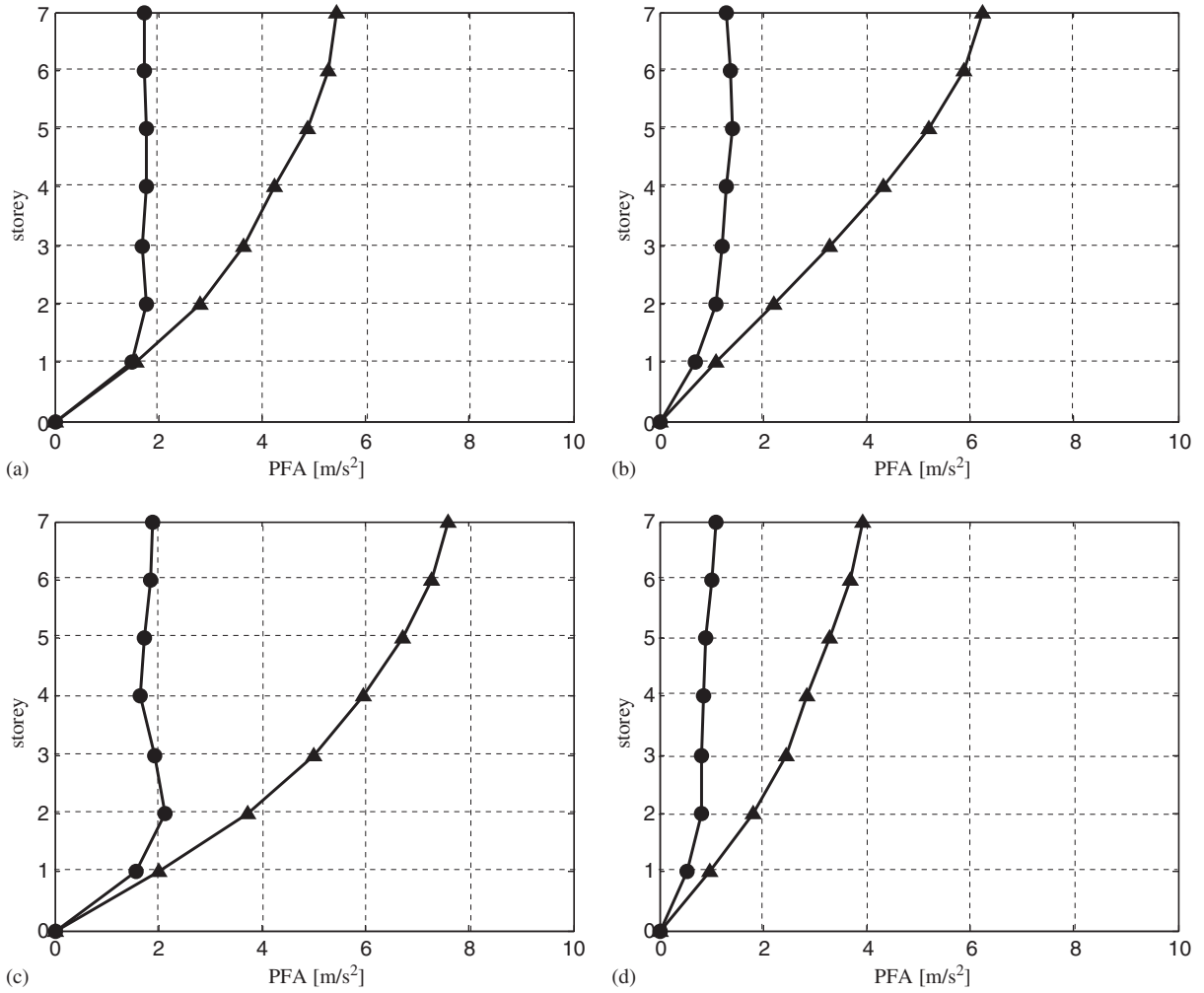

Fig. 13. Peak floor accelerations (PFA) developed by the seven-storey reference structure equipped with MPD system (—●—) and SPD system (—▲—) under the earthquakes: (a) Imperial Valley, 1940 (El Centro record, NS component 270°, PGA = 0.215 g), (b) Kern County, 1952 (Taft Lincoln School record, EW component 21°, PGA = 0.156 g), (c) Kobe, 1995 (Kobe University record, NS component 90°, PGA = 0.310 g), (d) Northridge, 1994 (Camarillo record, EW component 180°, PGA = 0.125 g).

12. Conclusions

The dynamic properties of mdof shear-type structures, characterised by constant values of lateral stiffness and floor mass, and equipped with manufactured viscous dampers that lead to Rayleigh damping matrices, are investigated in this paper.

The authors firstly identify that the mass proportional and stiffness proportional components of the Rayleigh damping systems correspond to two physically separated and independently implementable systems, here referred to as mass proportional damping (MPD) system and

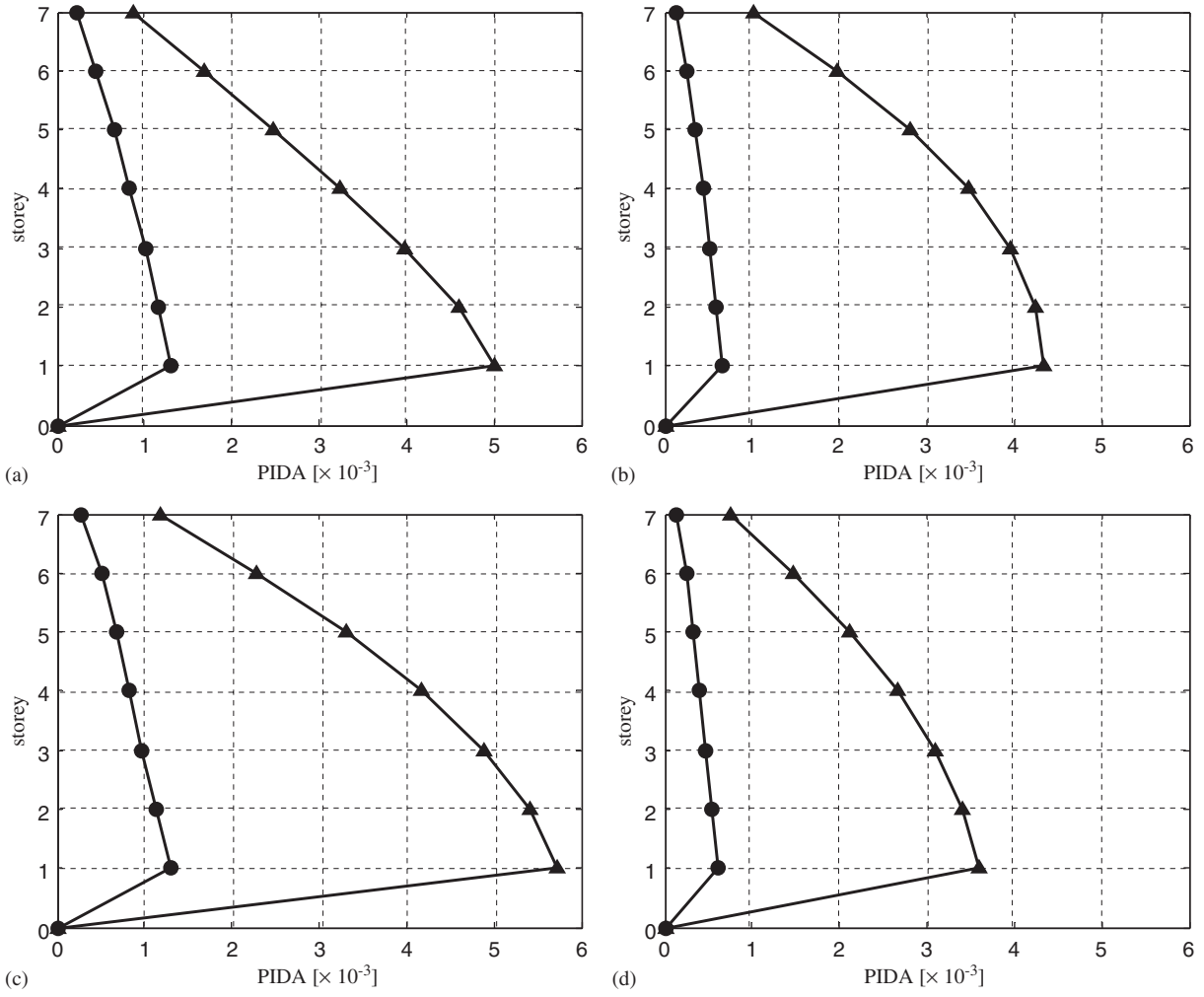

Fig. 14. Peak inter-storey drift angles (PIDA) developed by the seven-storey reference structure equipped with MPD system (—●—) and SPD system (—▲—) under the earthquakes: (a) Imperial Valley, 1940 (El Centro record, NS component 270°, PGA = 0.215 g), (b) Kern County, 1952 (Taft Lincoln School record, EW component 21°, PGA = 0.156 g), (c) Kobe, 1995 (Kobe University record, NS component 90°, PGA = 0.310 g), (d) Northridge, 1994 (Camarillo record, EW component 180°, PGA = 0.125 g).

stiffness proportional damping (SPD) system, respectively. These two systems being characterised by a specific and different damper placement.

Secondly, under the equal "total size" constraint (the total size being defined as the sum of the damping coefficients of all viscous dampers added to the structure), it is demonstrated here , from basic physics, that the first modal damping ratio provided by the MPD system, ξ_1^{MPD}, is always larger than the first modal damping ratio provided by the corresponding SPD system, ξ_1^{SPD}.

Demonstrations for an upper bound and a close approximation of the ratio $\xi_1^{\mathrm{SPD}}/\xi_1^{\mathrm{MPD}}$ as a function of the total number of storeys N are also provided herein and show that the ratio $\xi_1^{\mathrm{SPD}}/\xi_1^{\mathrm{MPD}}$ decreases with increasing N.

An exact close-form expression for the ratio between (a) the geometrical sum of all ξ_i^{MPD} and (b) the geometrical sum of all ξ_i^{SPD} is given herein and shows that this ratio increases with increasing N.

The results obtained are fundamental because they provide an analytical demonstration for the fact that shear-type structures equipped with MPD systems, when excited at the base, show, in general, a higher damping efficiency than structures equipped with equal "total size" SPD systems. This observation had been already identified by the authors in previous research works carried out through numerical simulations [17–20, 30] and is synthetically presented herein through an illustrative numerical example obtained with reference to a realistic seven-storey shear-type structure.

Acknowledgements

The authors gratefully acknowledge Prof. Cristina Fiocchi, Department of Pure and Applied Mathematics, University of Modena and Reggio Emilia, Italy, for her contributions.

Appendix. Demonstrations of partial results

This appendix provides detailed mathematical demonstrations for the partial results used in the demonstrations presented in this paper.

A.1. Demonstration that $p_N(\Lambda) = (2-\Lambda)p_{N-1}(\Lambda) - p_{N-2}(\Lambda)$

Let us now derive a recursive formula for the expression of the characteristic polynomial of the $N \times N$ matrix $\mathbf{A}_N$ as a function of the characteristic polynomials of the $(N-1) \times (N-1)$ matrix $\mathbf{A}_{N-1}$ and the $(N-2) \times (N-2)$ matrix $\mathbf{A}_{N-2}$.

The expression of the numerical matrix $\mathbf{A}_N$ given by Eq. (27) allows to express the characteristic polynomial of Eq. (30) in the following form:

$$p_N(\Lambda) = \det \underbrace{\begin{bmatrix} 2-\Lambda & -1 & 0 & \dots & & & 0 \\ -1 & 2-\Lambda & -1 & 0 & \dots & & 0 \\ 0 & -1 & 2-\Lambda & \dots & \dots & & \dots \\ \dots & 0 & \dots & \dots & & & \dots \\ & & \dots & & \dots & -1 & 0 \\ & & & & -1 & 2-\Lambda & -1 \\ 0 & \dots & & \dots & 0 & -1 & 1-\Lambda \end{bmatrix}}_{N \times N}. \tag{A.1}$$

By using the determinant rules, it follows that

$$p_N(\Lambda) = (2-\Lambda)(-1)^{1+1}\det\underbrace{\begin{bmatrix} 2-\Lambda & -1 & 0 & \dots & & & 0 \\ -1 & 2-\Lambda & -1 & 0 & \dots & & 0 \\ 0 & -1 & 2-\Lambda & \dots & \dots & & \dots \\ \dots & 0 & \dots & \dots & & & \dots \\ & & \dots & & \dots & -1 & 0 \\ & & & & -1 & 2-\Lambda & -1 \\ 0 & \dots & & \dots & 0 & -1 & 1-\Lambda \end{bmatrix}}_{(N-1)\times(N-1)}$$

$$+(-1)(-1)^{1+2}\det\underbrace{\begin{bmatrix} -1 & -1 & 0 & \dots & & & 0 \\ 0 & 2-\Lambda & -1 & 0 & \dots & & 0 \\ 0 & -1 & 2-\Lambda & \dots & \dots & & \dots \\ \dots & 0 & \dots & \dots & & & \dots \\ & & \dots & & \dots & -1 & 0 \\ & & & & -1 & 2-\Lambda & -1 \\ 0 & \dots & & \dots & 0 & -1 & 1-\Lambda \end{bmatrix}}_{(N-1)\times(N-1)}. \tag{A.2}$$

Eq. (A.2) can be rewritten as

$$p_N(\Lambda) = (2-\Lambda)p_{N-1}(\Lambda) + \det\underbrace{\begin{bmatrix} -1 & -1 & 0 & \dots & & & 0 \\ 0 & 2-\Lambda & -1 & 0 & \dots & & 0 \\ 0 & -1 & 2-\Lambda & \dots & \dots & & \dots \\ \dots & 0 & \dots & \dots & & & \dots \\ & & \dots & & \dots & -1 & 0 \\ & & & & -1 & 2-\Lambda & -1 \\ 0 & \dots & & \dots & 0 & -1 & 1-\Lambda \end{bmatrix}}_{(N-1)\times(N-1)}, \tag{A.3}$$

where $p_{N-1}(\Lambda) = \det(\mathbf{A}_{N-1} - \Lambda\mathbf{I}_{N-1})$. By developing the second term on the right-hand side of Eq. (A.3), it follows that

$$p_N(\Lambda) = (2-\Lambda)p_{N-1}(\Lambda) + (-1)(-1)^{1+1}\det\underbrace{\begin{bmatrix} 2-\Lambda & -1 & 0 & \ldots & & & 0 \\ -1 & 2-\Lambda & -1 & 0 & \ldots & & 0 \\ 0 & -1 & 2-\Lambda & \ldots & \ldots & & \ldots \\ \ldots & 0 & \ldots & \ldots & & & \ldots \\ & & \ldots & & \ldots & -1 & 0 \\ & & & & -1 & 2-\Lambda & -1 \\ 0 & \ldots & & \ldots & 0 & -1 & 1-\Lambda \end{bmatrix}}_{(N-2)\times(N-2)}. \tag{A.4}$$

In turn, Eq. (A.4) leads to Eq. (44) of the main text.

A.2. Expression for $a_{0,N}$

According to the notation of Eq. (31), $a_{0,N}$ is the term of degree 0 of the polynomial $p_N(\Lambda) = \det(\mathbf{A}_N - \Lambda\mathbf{I}_N)$ of Eq. (30), i.e. it is the value assumed by the polynomial for $\Lambda = 0$. Therefore, from Eq. (30):

$$a_{0,N} = p_N(0) = \det\ \mathbf{A}_N. \tag{A.5}$$

We want to prove that Eq. (32.1) holds for any value of N.

For the case $N = 2$:

$$a_{0,2} = p_2(0) = \det\ \mathbf{A}_2 = \det\begin{bmatrix} 2 & -1 \\ -1 & 1 \end{bmatrix} = 2 - 1 = 1. \tag{A.6}$$

For the case $N = 3$:

$$a_{0,3} = p_3(0) = \det\ \mathbf{A}_3 = \det\begin{bmatrix} 2 & -1 & 0 \\ -1 & 2 & -1 \\ 0 & -1 & 1 \end{bmatrix} = 4 - 2 - 1 = 1. \tag{A.7}$$

Let us now demonstrate that Eq. (32.1) is true by induction, i.e. if it is true for $N-1$ and for $N-2$ (hypotheses), then it is true also for N (thesis). Let us therefore assume as hypotheses the following:

$$\text{(hypothesis) } a_{0,N-1} = 1, \tag{A.8}$$

$$\text{(hypothesis) } a_{0,N-2} = 1. \tag{A.9}$$

Eqs. (44), (A.5), (A.8) and (A.9) lead to

$$a_{0,N} = p_N(0) = 2p_{N-1}(0) - p_{N-2}(0) = 2a_{0,N-1} - a_{0,N-2} = 2 \times 1 - 1 = 1 \tag{A.10}$$

which verifies the thesis of Eq. (32.1). Given that Eqs. (A.6) and (A.7) show that Eq. (32.1) is true for the two smallest considered N ($N = 2$ and 3), it follows that Eq. (32.1) holds for any value of N.

A.3. Expression for $a_{1,N}$

According to the notation of Eq. (31), $a_{1,N}$ is the multiplicative coefficient of the term of degree 1 of the polynomial $p_N(\Lambda) = \det(\mathbf{A}_N - \Lambda \mathbf{I}_N)$ of Eq. (30). We want to prove that Eq. (32.2) holds for any value of N.

For the case $N = 2$:

$$p_2(\Lambda) = \det\begin{bmatrix} 2-\Lambda & -1 \\ -1 & 1-\Lambda \end{bmatrix} = (2-\Lambda)(1-\Lambda) - 1 = 1 - 3\Lambda + \Lambda^2 \tag{A.11}$$

and therefore $a_{1,N} = a_{1,2} = -3$. In this case, Eq. (32.2) is verified as

$$a_{1,2} = -\frac{2(2+1)}{2} = -3. \tag{A.12}$$

For the case $N = 3$:

$$p_3(\Lambda) = \det\begin{bmatrix} 2-\Lambda & -1 & 0 \\ -1 & 2-\Lambda & -1 \\ 0 & -1 & 1-\Lambda \end{bmatrix} = 1 - 6\Lambda + 5\Lambda^2 - \Lambda^3 \tag{A.13}$$

and therefore $a_{1,N} = a_{1,3} = -6$. In this case, Eq. (32.2) is verified as

$$a_{1,3} = -\frac{3(3+1)}{2} = -6. \tag{A.14}$$

Let us now demonstrate that Eq. (32.2) is true by induction, i.e. if it is true for $N-1$ and for $N-2$ (hypotheses), then it is true also for N (thesis). Let us therefore assume as hypotheses the following:

$$\text{(hypothesis)} \quad a_{1,N-1} = -\tfrac{(N-1)N}{2}, \tag{A.15}$$

$$\text{(hypothesis)} \quad a_{1,N-2} = -\tfrac{(N-2)(N-1)}{2}. \tag{A.16}$$

From Eq. (44), the term of degree 1, $a_{1,N}\Lambda$, of the polynomial $p_N(\Lambda)$ can be seen as the sum of three contributions r_1, r_2 and r_3:

$$a_{1,N} = r_1 + r_2 + r_3, \tag{A.17}$$

where

- r_1 is equal to 2 multiplied by the coefficient of the term of degree 1 of the polynomial $p_{N-1}(\Lambda)$, i.e.

$$r_1 = 2a_{1,N-1} \tag{A.18}$$

which from Eq. (A.15) becomes

$$r_1 = 2\left(-\frac{(N-1)N}{2}\right). \tag{A.19}$$

- r_2 is equal to (-1) multiplied by the term of degree 0 of the polynomial $p_{N-1}(\Lambda)$, i.e.

$$r_2 = (-1)a_{0,N-1} \tag{A.20}$$

which from Eq. (32.1) becomes:

$$r_2 = (-1)1. \tag{A.21}$$

- r_3 is equal to (-1) multiplied by the coefficient of the term of degree 1 of the polynomial $p_{N-2}(\Lambda)$, i.e.

$$r_3 = (-1)a_{1,N-2} \tag{A.22}$$

which from Eq. (A.16) becomes

$$r_3 = (-1)\left(-\frac{(N-2)(N-1)}{2}\right). \tag{A.23}$$

From Eqs. (A.17), (A.19), (A.21) and (A.23):

$$a_{1,N} = -N(N-1) - 1 + \frac{(N-2)(N-1)}{2} = -\frac{N(N+1)}{2} \tag{A.24}$$

which verifies the thesis of Eq. (32.2). Given that Eqs. (A.12) and (A.14) show that Eq. (32.2) is true for the two smallest considered N ($N = 2$ and 3), it follows that Eq. (32.2) holds for any value of N.

A.4. Expression for $a_{N,N}$

According to the notation of Eq. (31), $a_{N,N}$ is the multiplicative coefficient of the term of degree N of the polynomial $p_N(\Lambda) = \det(\mathbf{A}_N - \Lambda\mathbf{I}_N)$ of Eq. (30). The term of degree N, $a_N\Lambda^N$, derives from the multiplication of all N diagonal terms (the only ones containing Λ). As in all diagonal terms Λ is multiplied by –1, it results that Eq. (32.3) holds for any value of N.

A.5. Expression for $a_{N-1,N}$

According to the notation of Eq. (31), $a_{N-1,N}$ is the multiplicative coefficient of the term of degree $N-1$ of the polynomial $p_N(\Lambda) = \det(\mathbf{A}_N - \Lambda\mathbf{I}_N)$ of Eq. (30). We want to prove that Eq. (32.4) holds for any value of N.

For the case $N = 2$:

$$p_2(\Lambda) = \det\begin{bmatrix} 2-\Lambda & -1 \\ -1 & 1-\Lambda \end{bmatrix} = (2-\Lambda)(1-\Lambda) - 1 = 1 - 3\Lambda + \Lambda^2 \tag{A.25}$$

and therefore $a_{N-1,N} = a_{1,2} = -3$. In this case, Eq. (32.4) is verified as

$$a_{1,2} = (-1)^{2-1}(2 \times 2 - 1) = -3. \tag{A.26}$$

Let us now demonstrate that Eq. (32.4) is true by induction, i.e. if it is true for $N-1$ (hypothesis), then it is true also for N (thesis). Let us therefore assume as hypothesis the following:

$$\text{(hypothesis)} \quad a_{(N-1)-1,(N-1)} = (-1)^{(N-1)-1}(2(N-1)-1). \tag{A.27}$$

The term of degree $N-1$, $a_{N-1,N}\Lambda^{N-1}$, of the polynomial of Eq. (44), comes only from the first term on the right-hand side of Eq. (44), i.e. from $(2-\Lambda)p_{N-1}(\Lambda)$, as the term with the highest degree of $p_{N-2}(\Lambda)$ is Λ^{N-2}.

In particular, the coefficient of the term of degree $N-1$ is the sum of the two contributions q_1 and q_2:

$$a_{N-1,N} = q_1 + q_2, \tag{A.28}$$

where

- q_1 is equal to 2 multiplied by the coefficient of the term of degree $N-1$ of the polynomial $p_{N-1}(\Lambda)$, i.e.

$$q_1 = 2a_{N-1,N-1} \tag{A.29}$$

  which from Eq. (32.3) becomes

$$q_1 = 2(-1)^{N-1}. \tag{A.30}$$

- q_2 is equal to (-1) multiplied by the coefficient of the term of degree $N-2$ of the polynomial $p_{N-1}(\Lambda)$, i.e.

$$q_2 = (-1)a_{N-2,N-1} \tag{A.31}$$

which from Eq. (A.27) becomes

$$q_2 = (-1)(-1)^{N-2}(2(N-1)-1). \tag{A.32}$$

From Eqs. (A.28), (A.30) and (A.32)

$$a_{N-1,N} = 2(-1)^{N-1} + (-1)(-1)^{N-2}(2(N-1)-1) = (-1)^{N-1}(2N-1) \tag{A.33}$$

which verifies the thesis of Eq. (32.4). Given that Eq. (A.26) shows that Eq. (32.4) is true for the smallest considered N ($N = 2$), it follows that Eq. (32.4) holds for any value of N.

A.6. Demonstration that $f'_N(\Lambda) > 0$

We want to prove that

$$\text{(thesis)} \quad f'_N(\Lambda) > 0. \tag{A.34}$$

Let us first verify Eq. (A.34) for the smallest value of N taken into consideration ($N = 2$):

$$f_2(\Lambda) = \frac{p_0(\Lambda)}{p_1(\Lambda)}. \tag{A.35}$$

From Eqs. (31), (32.1) and (32.2)

$$p_0(\Lambda) = 1 \quad \text{and} \quad p_1(\Lambda) = 1 - \Lambda \tag{A.36}$$

which lead to

$$f'_2(\Lambda) = \frac{1}{(1-\Lambda)^2} \tag{A.37}$$

which is larger than zero for any value of Λ.

Let us now demonstrate that Eq. (A.34) is true by induction, i.e. if it is true for $N-1$ (hypothesis), then it is true also for N (thesis). Let us therefore assume as hypothesis the following:

$$\text{(hypothesis)} \quad f'_{N-1}(\Lambda) > 0. \tag{A.38}$$

From Eqs. (43) and (44)

$$\begin{aligned} f_N(\Lambda) &= \frac{p_{N-2}(\Lambda)}{p_{N-1}(\Lambda)} = \frac{1}{\frac{p_{N-1}(\Lambda)}{p_{N-2}(\Lambda)}} = \frac{1}{\frac{(2-\Lambda)p_{N-2}(\Lambda) - p_{N-3}(\Lambda)}{p_{N-2}(\Lambda)}} \\ &= \frac{1}{(2-\Lambda) - \frac{p_{N-3}(\Lambda)}{p_{N-2}(\Lambda)}} = \frac{1}{(2-\Lambda) - f_{N-1}(\Lambda)} \end{aligned} \tag{A.39}$$

and

$$f'_N(\Lambda) = \frac{1 + f'_{N-1}(\Lambda)}{\left[(2-\Lambda) - f_{N-1}(\Lambda)\right]^2} \tag{A.40}$$

which, given the hypothesis of Eq. (A.38), is larger than zero for any value of Λ, thus verifying the thesis of Eq. (A.34). Given that Eq. (A.37) shows that Eq. (A.34) is true for the smallest considered N ($N = 2$), it follows that Eq. (A.34) holds for any value of N.

A.7. Demonstration that $f''_N(\Lambda) > 0$ for $\Lambda \in (0, \Lambda_{1,N-1})$

We want to prove that

$$\text{(thesis)} \quad f''_N(\Lambda) > 0 \quad \text{for } \Lambda \in \left(0, \Lambda_{1,N-1}\right). \tag{A.41}$$

Let us first verify Eq. (A.41) for the smallest value of N taken into consideration ($N = 2$). From Eq. (A.37)

$$f''_2(\Lambda) = \frac{2}{(1-\Lambda)^3} \tag{A.42}$$

which is larger than zero for $\Lambda \in (0,1)$. Given that from Eq. (A.36) $\Lambda_{1,1} = 1$, the thesis of Eq. (A.41) is verified.

Let us now demonstrate that Eq. (A.41) is true by induction, i.e. if it is true for $N-1$ (hypothesis), then it is true also for N (thesis). Let us therefore assume as hypothesis the following:

$$\text{(hypothesis)} \quad f''_{N-1}(\Lambda) > 0 \quad \text{for } \Lambda \in \left(0, \Lambda_{1,N-2}\right). \tag{A.43}$$

From Eq. (A.40)

$$f''_N(\Lambda) = t_1(\Lambda) + t_2(\Lambda), \tag{A.44}$$

where

$$t_1(\Lambda) = \frac{2\left(1 + f'_{N-1}(\Lambda)\right)^2}{\left((2-\Lambda) - f_{N-1}(\Lambda)\right)^3} \tag{A.45}$$

and

$$t_2(\Lambda) = \frac{f''_{N-1}(\Lambda)}{\left((2-\Lambda) - f_{N-1}(\Lambda)\right)^2}. \tag{A.46}$$

$t_1(\Lambda) > 0$ if $(2-\Lambda) - f_{N-1}(\Lambda) > 0$, which corresponds to

$$g(\Lambda) > f_{N-1}(\Lambda). \tag{A.47}$$

Given that $g(0) = 2$ and $f_{N-1}(0) = 1$ and that, by definition, the first intersection between $g(\Lambda)$ and $f_{N-1}(\Lambda)$ occurs at $\Lambda = \Lambda_{1,N-1}$, it follows that [29]

$$g(\Lambda) > f_{N-1}(\Lambda) \quad \text{for } \Lambda \in \left(0, \Lambda_{1,N-1}\right) \tag{A.48}$$

which implies

$$t_1(\Lambda) > 0 \quad \text{for } \Lambda \in \left(0, \Lambda_{1,N-1}\right). \tag{A.49}$$

Given the hypothesis of Eq. (A.43), $t_2(\Lambda) > 0$ for $\Lambda \in \left(0, \Lambda_{1,N-2}\right)$ and, due to Eq. (45), all the more reason

$$t_2(\Lambda) > 0 \quad \text{for } \Lambda \in \left(0, \Lambda_{1,N-1}\right). \tag{A.50}$$

From Eqs. (A.44), (A.49) and (A.50), the thesis of Eq. (A.41) is verified. Given that Eq. (A.42) shows that Eq. (A.41) is true for the smallest considered N ($N = 2$), it follows that Eq. (A.41) holds for any value of N.

A.8. Demonstration that $f'_N(0) = N - 1$

We want to prove that

$$\text{(thesis)} \quad f'_N(0) = N - 1\,. \tag{A.51}$$

Let us first verify Eq. (A.51) for the smallest value of N taken into consideration ($N = 2$). From Eq. (A.37)

$$f'_2(0) = 1 \tag{A.52}$$

which verifies the thesis of Eq. (A.51).

Let us now demonstrate that Eq. (A.51) is true by induction, i.e. if it is true for $N-1$ (hypothesis), then it is true also for N (thesis). Let us therefore assume as hypothesis the following:

$$\text{(hypothesis)} \quad f'_{N-1}(0) = (N-1) - 1 = N - 2. \tag{A.53}$$

From Eqs. (A.40), (A.53) and given that $f_{N-1}(0) = 1$

$$f'_N(0) = \frac{1 + N - 2}{[2-1]^2} = N - 1 \tag{A.54}$$

which verifies the thesis of Eq. (A.51). Given that Eq. (A.52) shows that Eq. (A.51) is true for the smallest considered N ($N = 2$), it follows that Eq. (A.51) holds for any value of N.

References

[1] G.C. Hart, K. Wong, *Structural Dynamics for Structural Engineers*, Wiley, New York, 2000.

[2] http://nisee.berkeley.edu/prosys.html.

[3] H. Li, S.Y. Wang, G. Song, G. Liu, Reduction of seismic forces on existing buildings with newly constructed additional storeys including friction layer and dampers, *Journal of Sound and Vibration* 269 (2004) 653–667.

[4] R.H. Zhang, T.T. Soong, Seismic design of viscoelastic dampers for structural applications, *Journal of Structural Engineering ASCE* 118 (5) (1992) 1375–1392.

[5] I. Takewaki, Optimal damper placement for minimum transfer functions, *Earthquake Engineering and Structural Dynamics* 26 (1997) 1113–1124.

[6] I. Takewaki, Optimal damper placement for critical excitation, *Probabilistic Engineering Mechanics* 15 (2000) 317–325.

[7] M.P. Singh, L.M. Moreschi, Optimal seismic response control with dampers, *Earthquake Engineering and Structural Dynamics* 30 (2001) 553–572.

[8] M.P. Singh, L.M. Moreschi, Optimal placement of dampers for passive response control, *Earthquake Engineering and Structural Dynamics* 31 (2002) 955–976.

[9] J.A. Main, S. Krenk, Efficiency and tuning of viscous dampers on discrete systems, *Journal of Sound and Vibration* 286 (2005) 97–122.

[10] http://www.kisho.co.jp/WorksAndProjects/Works/kaigi/.

[11] http://www.arup.com/dyna/applications/seismic/seismic.htm.

[12] http://www.bennettbldg.com.

[13] P.W. Clark, I.D. Aiken, E. Ko, K. Kasai, I. Kimura, Design procedures for building incorporating hysteretic damping devices, *Proceedings of the 68th Annual Convention, Structural Engineers Association of California*, Santa Barbara, CL, 1999.

[14] P. Brown, I.D. Aiken, F.J. Jafarzadeh, Seismic Retrofit of the W. F. Bennett Federal Building, *Modern Steel Construction*, 2001, http://www.aisc.org/msc/0108_03_seismicretrofit.pdf.

[15] R.W. Clough, J. Penzien, *Dynamics of Structures*, second ed, McGraw-Hill, New York, Civil Engineering Series, International Editions, 1993.
[16] A.K. Chopra, *Dynamics of Structures. Theory and Applications to Earthquake Engineering*, Prentice-Hall, Upper Saddle River, NJ, 1995.
[17] S. Silvestri, T. Trombetti, C. Ceccoli, Inserting the mass proportional damping (MPD) system in a concrete shear-type structure, *Structural Engineering and Mechanics* 16 (2) (2003) 177–193.
[18] T. Trombetti, S. Silvestri, Added viscous dampers in shear-type structures: the effectiveness of mass proportional damping, *Journal of Earthquake Engineering* 8 (2) (2004) 275–313.
[19] S. Silvestri, T. Trombetti, C. Ceccoli, An innovative damping scheme for shear-type structures: the MPD system, *Proceedings of the Second International Speciality Conference on The Conceptual Approach to Structural Design*, vol. 2, CDS-03, Milano Bicocca, Italy, July 2003, pp. 789–796, ISBN: 981-04-8561-1.
[20] S. Silvestri, T. Trombetti, C. Ceccoli, Optimal insertion of viscous dampers into shear-type structures: seismic performances and applicability of the MPD system, *Proceedings of the 13th World Conference on Earthquake Engineering*, 13WCEE, Vancouver, BC, Canada, August 1–6, 2004, Paper no. 477.
[21] W.S. Zhang, Y.L. Xu, Vibration analysis of two buildings linked by Maxwell model-defined fluid dampers, *Journal of Sound and Vibration* 233 (5) (2000) 775–796.
[22] Y.Q. Ni, J.M. Ko, Random seismic response analysis of adjacent buildings coupled with non linear hysteretic dampers, *Journal of Sound and Vibration* 246 (3) (2001) 403–417.
[23] T. Aida, T. Aso, K. Takeshita, T. Takiuchi, T. Fujii, Improvement of the structure damping performance by interconnection, *Journal of Sound and Vibration* 242 (2) (2001) 333–353.
[24] M.R. Casali, C. Gagliardi, L. Grasselli, *Geometria*, Progetto Leonardo, Società Editrice Esculapio, Bologna, 2001.
[25] C. Gagliardi, L. Grasselli, *Algebra Lineare e Geometria. Parte Prima*, Progetto Leonardo, Società Editrice Esculapio, Bologna, 1992.
[26] C. Gagliardi, L. Grasselli, *Algebra Lineare e Geometria. Parte Terza*, Progetto Leonardo, Società Editrice Esculapio, Bologna, 1993.
[27] T.M. Apostol, *Calcolo. Volume Secondo: Geometria*, Boringhieri Editore, Torino, 1977.
[28] C. Citrini, *Analisi Matematica I*, first ed., Bollati Boringhieri Editore, Torino, 1991.
[29] G.C. Barozzi, S. Matarasso, *Analisi Matematica I*, first ed, N. Zanichelli Editore, Bologna, 1986.
[30] S. Silvestri, T. Trombetti, Optimal insertion of viscous dampers into shear-type structures: dissipative properties of the MPD system. *Proceedings of the 13th World Conference on Earthquake Engineering*, 13WCEE, Vancouver, BC, Canada, August 1–6, 2004, Paper no. 473.